A Review on CO2 Capture Technologies with Focus on CO2-Enhanced Methane Recovery from Hydrates

energies

MDPI

Review

A Review on CO_2 Capture Technologies with Focus on CO_2-Enhanced Methane Recovery from Hydrates

Salvatore F. Cannone *, Andrea Lanzini and Massimo Santarelli

Energy Department, Politecnico di Torino, Via Duca degli Abruzzi 24, 10129 Torino, Italy; andrea.lanzini@polito.it (A.L.); massimo.santarelli@polito.it (M.S.)
* Correspondence: salvatore.cannone@polito.it

Abstract: Natural gas is considered a helpful transition fuel in order to reduce the greenhouse gas emissions of other conventional power plants burning coal or liquid fossil fuels. Natural Gas Hydrates (NGHs) constitute the largest reservoir of natural gas in the world. Methane contained within the crystalline structure can be replaced by carbon dioxide to enhance gas recovery from hydrates. This technical review presents a techno-economic analysis of the full pathway, which begins with the capture of CO_2 from power and process industries and ends with its transportation to a geological sequestration site consisting of clathrate hydrates. Since extracted methane is still rich in CO_2, on-site separation is required. Focus is thus placed on membrane-based gas separation technologies widely used for gas purification and CO_2 removal from raw natural gas and exhaust gas. Nevertheless, the other carbon capture processes (i.e., oxy-fuel combustion, pre-combustion and post-combustion) are briefly discussed and their carbon capture costs are compared with membrane separation technology. Since a large-scale Carbon Capture and Storage (CCS) facility requires CO_2 transportation and storage infrastructure, a technical, cost and safety assessment of CO_2 transportation over long distances is carried out. Finally, this paper provides an overview of the storage solutions developed around the world, principally studying the geological NGH formation for CO_2 sinks.

Keywords: carbon capture and storage (CCS); CO_2 replacement; CO_2 capture; CO_2 transportation; CO_2 storage; natural gas; gas hydrate; sustainability; membrane technology; economic analysis

Citation: Cannone, S.F.; Lanzini, A.; Santarelli, M. A Review on CO_2 Capture Technologies with Focus on CO_2-Enhanced Methane Recovery from Hydrates. *Energies* **2021**, *14*, 387. https://doi.org/10.3390/en14020387

Received: 23 October 2020
Accepted: 8 January 2021
Published: 12 January 2021

1. Introduction

The processing of raw materials, energy production, and human activity in general has caused a rise in the temperature of about 1.0 °C above pre-industrial levels, leading to climate change at a global level. The risks for natural and human systems are obviously even higher for global warming of 1.5 °C, but still lower than in the case of a rise of 2.0 °C. Limiting global warming to 1.5 °C reduces the impacts on ocean and terrestrial ecosystems, health, food safety, water supply, and economic growth compared to 2.0 °C [1].

Global energy consumption in 2018 increased by 2.3% with respect to 2017 scenarios due to economic improvement and a higher heating and cooling requirement in some regions of the world. The increase in energy efficiency and the share of renewable energy, and the transition from coal to gas power plants, have helped to avoid a lot of CO_2 emissions. Nevertheless, the CO_2 emissions rose by 1.7%, reaching a total of 33.1 Gigatons (Gt). This means that energy consumption and CO_2 emissions increase together, and they are not yet decoupled. The largest CO_2 emitter, accounting for 30% of carbon dioxide emissions related to energy consumption, is coal-fired power generation. The growing energy demand is not totally covered by new renewable plants and, consequently, fossil fuel consumption is increasing (e.g., the consumption of natural gas rose by 4.6% in 2018) [2].

Natural gas, composed mostly of methane, is considered a helpful bridge fuel to reduce the greenhouse gas emissions of fossil fuels. It has the lowest carbon intensity (i.e., the emission rate of a given pollutant relative to a specific activity), emitting less

CO_2 per unit of energy generated than other fossil fuels. It burns cleanly and efficiently, and generally requires limited processing to prepare it for end-users, with lower carbon emissions in comparison to other fuels. However, the energy density of natural gas at environmental condition (i.e., between 38.15 and 40.72 MJ/m^3) is lower than that of liquid petroleum fuels, which have an energy density range of 28,000 to 42,000 MJ/m^3 [3]. As a result, the transportation and storage of gas fuel require a compression or liquefaction step to obtain the same quantity of energy over the same volume of liquid fuels.

The possible solutions leading to the reduction of CO_2 emissions are: (i) switching to a low carbon economy; (ii) increasing system efficiency; (iii) implementing CCS technologies to allow a gradual transition from fossil fuels to other more sustainable ones. Renewable power plants cannot provide enough base-load electricity generation, and they depend on geographical location and, therefore, on the availability of resources. Thus, CCS is a feasible solution to reduce the anthropogenic CO_2 emissions in a transition phase [4].

Thermogenic natural gas is formed when buried organic material is subjected to enormous heat and pressure over geological time. Natural gas reservoirs are categorised as conventional or unconventional gas reserves. Conventional resources of natural gas are accumulated in permeable rocks comprising of numerous pores which allow them to retain natural gas. This gas is trapped underground by impermeable rock strata. Natural gas can be extracted economically without specialised technologies, using vertical well bores [5]. Otherwise, unconventional resources are formed in more complex geological formations (e.g., shale gas and tight gas), trapped in rocks with lower porosity and permeability than conventional reservoirs. These rocks prevent the easy flow of the gas through the pores to the standard type of well. The extraction of gas from these reservoirs requires expensive specialised techniques, such as hydraulic fracturing [5]. NGHs are deposited both in continental sedimentary rocks, in the polar area, and marine sediments, and they form at low temperatures ($\leq$26.85 °C) and moderate/high pressure ($\geq$6 bar) [6]. Clathrate hydrates are solid crystalline compounds in which, typically, methane, ethane, propane and carbon dioxide are trapped inside cages of water molecules.

This work is part of a larger research project aims to develop an innovative technological solution to enhance the extraction of subsea methane from marine NGHs. CO_2 is injected in subsea NGH formations to enhance methane recovery and is eventually trapped as stable gas hydrates in a substitution process. As a result, the fuel obtained is virtually neutral in terms of GHG emissions.

The replacement of CH_4 with CO_2 is thermodynamically favoured, and it represents a unique opportunity to recover an energy resource and to store this common greenhouse gas. Therefore, geological NGH formation can be used as an energy resource, capable of providing methane, whilst CO_2 storage could contribute to reducing GHG emissions.

In this paper we review the current state-of-the-art of CO_2 capture, transport and storage, focusing on hydrate storage at techno-economic level. We first discuss carbon capture processes applied to the industrial and power sector (Section 2), and highlight the CO_2 capture costs and performance of different power plants (Section 3). Then in Section 4 we contextualise CO_2 transportation via pipeline, neglecting other means of transport because they are less used. The sequestration of CO_2 is more widespread than its reuse, therefore, conventional CO_2 storage (e.g., brine aquifer and depleted oil and gas) and, in particular, clathrate hydrate formation are presented in Section 5. Section 6 concludes with the cost of the complete CCS process at different distances between the CO_2 source and sink, identifying one of the possible final CCS chains.

2. CO_2 Capture Systems

Many abatement technologies affect the use of fossil fuels or their emissions in the atmosphere (e.g., carbon capture, utilisation, and storage, use of nuclear power, replacement of coal by natural gas). CCS can be applied in power plants and industrial facilities and involves CO_2 separation, compression, and transportation (via pipeline or shipping) and its storage in a geological site (e.g., saline aquifer, oil and/or gas reservoir).

Therefore, the first step of CCS technology is sequestering CO_2, and the main carbon capture processes, summarized in Figure 1, are the following:

- Oxyfuel combustion: fuel is burnt with pure oxygen instead of air, and if it is free of contaminants, the resulting flue gas contains only carbon dioxide and water, easily separated by a water condenser.
- Pre-combustion: fuel is processed in a gasifier reactor to produce a syngas rich in hydrogen and carbon monoxide. Subsequently, this syngas flows into a water gas shift reactor to produce H_2 and CO_2. The final process provides CO_2 separation and pure hydrogen production usually via physical absorption.
- Post-combustion: the flue gas produced by conventional fuel combustion flows into a CO_2 separation unit. The procedures used to sequestrate the CO_2 are typically absorption by the aid of a chemical solvent, adsorption, and membrane separation.

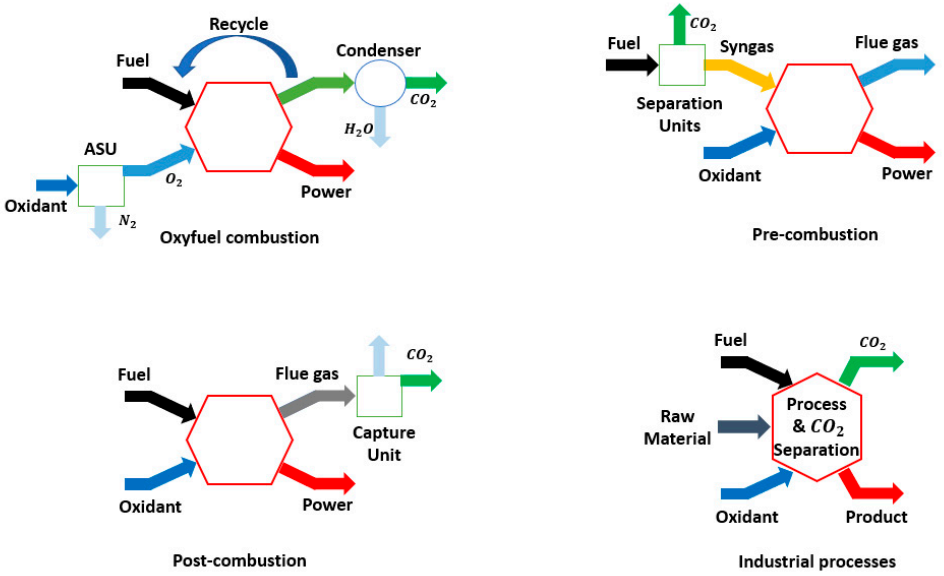

Figure 1. Schematic diagrams of carbon capture processes showing oxyfuel combustion, pre-combustion, and post-combustion applied to the energy sector, while the last diagram illustrates a general CO_2 separation process for a net-zero industry.

2.1. Decarbonization of Industrial Sector

Industry covers around 25% of the economic sector in terms of global Gross Domestic Product (GDP) [7] and produced 7.8 Gt of CO_2 in 2017 [8]. The Intergovernmental Panel on Climate Change (IPCC) states that direct and indirect (i.e., derived from energy use) emissions have to drop by 75–90% by 2050 [1]. CCS can be essential for industry decarbonisation, helping it to move toward sustainable mills. Nowadays, CCS technologies are mainly applied in the cement, steel and iron industries, and petrochemical and oil refining.

The cement industry contributes with 8% of global CO_2 emissions [9]. The emissions of CO_2 are mainly due to fuel combustion and the calcination of limestone (i.e., the main raw material for cement production). A new pilot plant called Low Emissions Intensity Lime and Cement (LEILAC) has been developed to capture over 95% of the CO_2 emissions. The key innovation of this plant is the high temperature direct separation calciner that can separate the CO_2 produced by the calcination reaction of the limestone [10].

The World Steel Association provides the mean value of carbon intensity, estimated to be 1.85 tonnes of CO_2 per tonnes of crude steel cast in 2018 [11], and, for the same year, states that the crude steel produced amounted to 1808 million tonnes [12]. Therefore, the iron and steel industry is one of the biggest emitters in industrial sectors, producing 3.3 Gt of CO_2 in 2018. Most iron and steel mills are made up of a Blast Furnace (BF) coupled with a Basic Oxygen Furnace (BOF), and they are supplied with iron ore as the raw material and coke as the reducing agent. To produce one ton of liquid steel (tLS), 1.81 t_{CO2} are

emitted into the atmosphere [13]. Conversely, new iron and steel mills, such as the one in Abu Dhabi, are being built with a new configuration. The main components of these plants are a Direct Reduction Iron (DRI) reactor coupled with an Electric Arc Furnace (EAF). Methane replaces coal and flows into a Steam Reformer (SR). The reducing gases produced and a mix of scrap and iron ore are conveyed into the DRI reactor. Hydrogen and carbon monoxide reduce the iron and CO_2 can be easily separated. At the end of this process, only 0.54 t_{CO2}/tLS are produced, saving 70% of CO_2 emissions [13].

Several large-scale CCS facilities applied to oil refining, fuel processing and fertiliser production are in operation. Most of them are in the USA (e.g., Illinois industrial CCS for Ethanol production, Century plant natural gas facility in Texas, Coffeyville gasification plant producing fertiliser) and CO_2 is transported from them for Enhanced Oil Recovery (EOR).

2.2. Decarbonization of the Power Sector

Electric power plants emit the largest of CO_2 into atmosphere. In the world several countries are primarily dependent upon coal-fired power plants. The first Super-Critical Pulverised Coal (SCPC) fired power plant (i.e., Philo unit 6) was built in 1957 and has been operated until the 1979 [14], while the first Ultra Super-Critical (USC) power plant was built in 1993 in Japan [15]. SCPC and USC power plants work at higher temperatures and pressure than a subcritical power plant. As a result, they achieve a higher thermodynamic efficiency. Coal is milled and burned with air (or near pure oxygen in case of oxy-fuel combustion carbon capture process) in the boiler. The heat produced by combustion is transferred to a secondary working fluid, typically water that circulates into a Rankine cycle. The steam operation conditions are above critical point (i.e., pressure 22.115 MPa and temperature 374.15 °C) and, at this state, there is no distinction between gas and liquid phase. In SCPC, steam is produced at pressure between 22.115 and 25 MPa and a temperature between 540–580 °C. In contrast, in USC power plant, water operates at pressure and temperature higher than 25 MPa and 580 °C, respectively [16]. The steam produced goes into turbines, which turns a shaft that is connected to a generator to generate electricity. The spent steam is condensed, and it flows again into the boiler.

There are only two large-scale facilities currently in operation based on post-combustion process Boundary Dam and Petra Nova coal-fired power plants are provided by a new separation unit (i.e., amine-based gas separation) used to purified the flue gas from SO_2 and NO_x, and separate the CO_2 from gas mixture [17,18]. Another large-scale CCS facility is in construction (i.e., the ZERO project) and it captures CO_2 with an oxy-fuel process. At the end, several pilot demonstration CCS facilities operate since 2010.

In the next sections, a techno-economic review is provided, showing the carbon capture cost of the different CCS processes applied to power plants.

3. Techno-Economic Considerations on CO_2 Capture

The minimum thermodynamic energy demand to separate one mole of CO_2 from a gas mixture is function of the CO_2 capture fraction (capture rate/100), and it is calculated through Equation (1). The equation below, provided by Amel'kin et al., considers the more realistic incomplete separation of CO_2, producing a pure stream of carbon dioxide and lean CO_2 flue gas [19].

$$W = -RT\left\{\ln\left[\frac{(1-f)x}{1-fx}\right] + \frac{\ln(1-fx)}{fx} - \frac{\ln(1-f)}{f}\right\} \quad (1)$$

where R is the specific gas constant (8.314 J/(mol K)), T is the temperature (K), x is the CO_2 mole fraction, and f is the CO_2 capture rate. Figure 2 shows the specific energy requirement for CO_2 separation as a function of the capture rate. Figure illustrates several CO_2 inlet concentrations that represent capture from air (410 ppm), natural gas combined cycle (4%), coal-fired power station (12%), and EAF steel plant (20%).

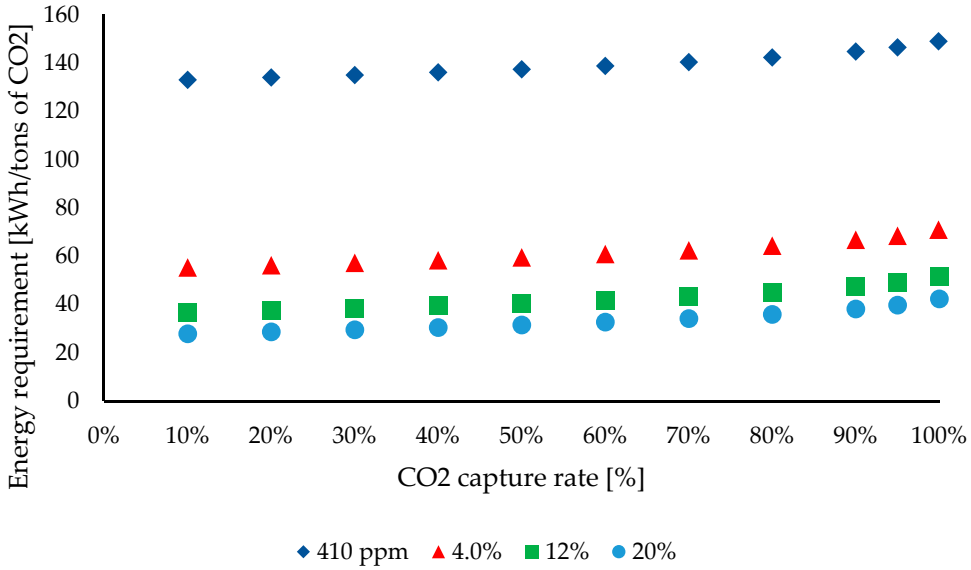

Figure 2. Minimum energy requirement for CO_2 capture depending on the capture rate and inlet concentration of CO_2 at 50 °C. $W = -RT\left\{\ln\left[\frac{(1-f)x}{1-fx}\right] + \frac{\ln(1-fx)}{fx} - \frac{\ln(1-f)}{f}\right\}$ [19].

The minimum energy requirement increases at high CO_2 capture rate and at low inlet concentration. Nevertheless, the energy demand in a real process is always higher.

The cost of CCS is the major challenge of this technology. The price of CCS is divided into three categories (capture, compression and transportation, and storage) as reported in the next section. The CCS cost is hard to estimate, mainly due to a lack of empirical data, different operating conditions and capture processes, and different CCS plants.

The cost of CCS [20] is often expressed as an energy (power generation sector) or efficiency (both power and industrial sectors) penalty. The energy penalty and efficiency penalty are represented below:

$$\text{Energy penalty} = 100 \cdot \frac{\text{Power output without CCS} - \text{Power output with CCS}}{\text{Power output without CCS}} \quad (2)$$

$$\text{Efficiency penalty} = \text{Efficiency without CCS} - \text{Efficiency with CCS [\%]} \quad (3)$$

For the power sector, another important parameter is the Levelized Cost of Electricity (LCOE) based on [$/MWh]. The electricity cost is evaluated as follows:

$$\text{LCOE} = \frac{\text{TCC} \cdot \text{FCF} + \text{FOM}}{\text{CF} \cdot 8766 \cdot \text{MW}} + \text{VOM} + \text{HR} \cdot \text{FC} \left[\frac{\$}{\text{MWh}}\right] \quad (4)$$

where: TCC is the Total Capital Cost [$]; FCF is the Fixed Charge Factor [fraction/year]; FOM is the Fixed Operating and Maintenance cost [$/year]; CF is the plant Capacity Factor; MW is the net plant capacity [MW]; VOM is the Variable non-fuel Operating and Maintenance cost [$/MWh]; HR is the net power plant Heat Rate [MJ/MWh]; FC is the unit Fuel Cost [$/MJ].

The various capture technologies are also compared by considering the cost of carbon, which may refer to both the CO_2 captured and CO_2 avoided costs in [$/t CO_2] shown in the equations below:

$$\text{Cost of captured } CO_2 = \frac{\text{LCOE}_{CC} - \text{LCOE}_{ref}}{\left(t_{CO_2}/\text{MWh}\right)_{captured}} \left[\frac{\$}{t_{CO_2}}\right] \quad (5)$$

$$\text{Cost of avoided } CO_2 = \frac{\text{LCOE}_{CCS} - \text{LCOE}_{ref}}{Q_{e,b} \cdot \left(1 - \frac{\eta_b}{\eta_{CC}} \cdot (1 - C)\right)} \left[\frac{\$}{t_{CO_2}}\right] \quad (6)$$

where $Q_{e,b}$ is the baseline emission [t_{CO2}/MWh], η_b—the baseline efficiency, η_{CC}—the efficiency with carbon capture, and C—the capture fraction. In future, the cost of CO_2 capture is likely to go down, but the estimation of future costs is rather uncertain.

Rubin et al. [21] reported the capture cost in constant 2013 US$, whereas Merkel et al. [22] reported the capture cost with membrane separation in constant 2011 US$. In this review, we report the overall cost of CSS in 2013 US$, and therefore the costs reported in different years have to be adjusted. We have used the Power Capital Cost Index (PCCI) to escalate the capital and non-fuel operating and maintenance costs of power plants, the fuel cost index to escalate the cost of coal and natural gas, and the Chemical Engineering Plant Cost Index (CEPCI) to escalate both the transportation and storage costs shown in Sections 4 and 5. In addition, the analysis reported in this work was performed using the First-Of-A-Kind (FOAK) CCS cost estimation, and therefore we have avoided all analyses which forecast a CCS cost reduction.

3.1. Oxy-Fuel Combustion CO_2 Capture

Oxyfuel combustion is one of the most mature technologies for capturing CO_2 from power plants. Near-pure oxygen is used as an oxidant to burn fuel. A fraction of flue gas composed almost entirely of CO_2, H_2, and oxygen in excess, is recirculated into the boiler to control the temperature in the combustion zone. Indeed, fuel combustion with pure O_2 produces a high adiabatic flame temperature. The separation of CO_2 occurs through dehydration of the flue gas at low temperatures. The flue gas may be purified of contaminants (e.g., SOx, NOx, HCl coming from the fuel and N_2, Ar, O_2 coming from the oxygen flow).

While the concentration of CO_2 of conventional coal-fired power plants is approximately 12%v, for a traditional gas turbine the content of carbon molecule is lower (about 4%v) due to the high excess of air used to control the combustion temperature. Therefore, post-combustion capture (via chemical adsorption) is disadvantaged, and oxyfuel combustion can be a good strategy [23].

Generally, these plants are classified in:

- Secondary cycle: flue gas, coming from the combustion chamber, heats an external working fluid through heat exchangers (e.g., Rankine cycles).
- Direct cycle: flue gas is also the working fluid and generates power in a turbo-gas (e.g., Brayton cycles).

The main components of oxyfuel combustion power generation are [23]: (i) Air Separation Unit (ASU) to produce near pure oxygen; (ii) Boiler or gas turbine to burn fuel and to generate power heat; (iii) Flue gas processing unit to clean flue gas and control its quality; (iv) CO_2 Processing Unit (CPU) for the final purification of carbon dioxide.

The main requirement for any oxyfuel combustion process is oxygen production. Conventional cryogenic multi-column distillation is currently the most efficient and cost-effective technology for producing oxygen on a large scale. The standard method consists of a double column distillation cycle with a high/low-pressure column. The gaseous air coming into a high-pressure column is separated into an overhead nitrogen vapor and oxygen-enriched bottom liquid. At the current plant size, the production of O_2, at 95% of purity and low pressure, consumes 200–250 kWh_{el}/t_{O_2} [23].

Oxyfuel combustion is applied both in coal-fired power plants and gas turbine-based power plants. In Figure 3a, the heat generated by coal combustion with near pure oxygen is supplied to a secondary cycle in the boiler. By contrast, in the gas turbine cycle shown in Figure 3b, the flue gas at high pressure and temperature produces electricity through a gas turbine (direct cycle) and provides power heat to a secondary cycle in a Heat Recovery Steam Generator (HRSG).

It is worth mentioning an emerging power plant based on the Allam cycle. The Allam cycle combines the oxy-combustion CO_2 capture process with the supercritical CO_2 used as working fluid at very high pressure ($\simeq$300 bar) and temperatures ($\simeq$1150 °C at the turbine

inlet). An Allam cycle power plant fueled by natural gas achieves 59% LHV efficiency and captures 100% of CO_2.

Before CO_2 storage or recirculation, the flue gas produced in a coal-fired power plant passes through several cleaner units to remove contaminants contained in the fuel. The contaminants are usually more numerous in coal than in gas fuel, and therefore more steps are needed to obtain useful CO_2.

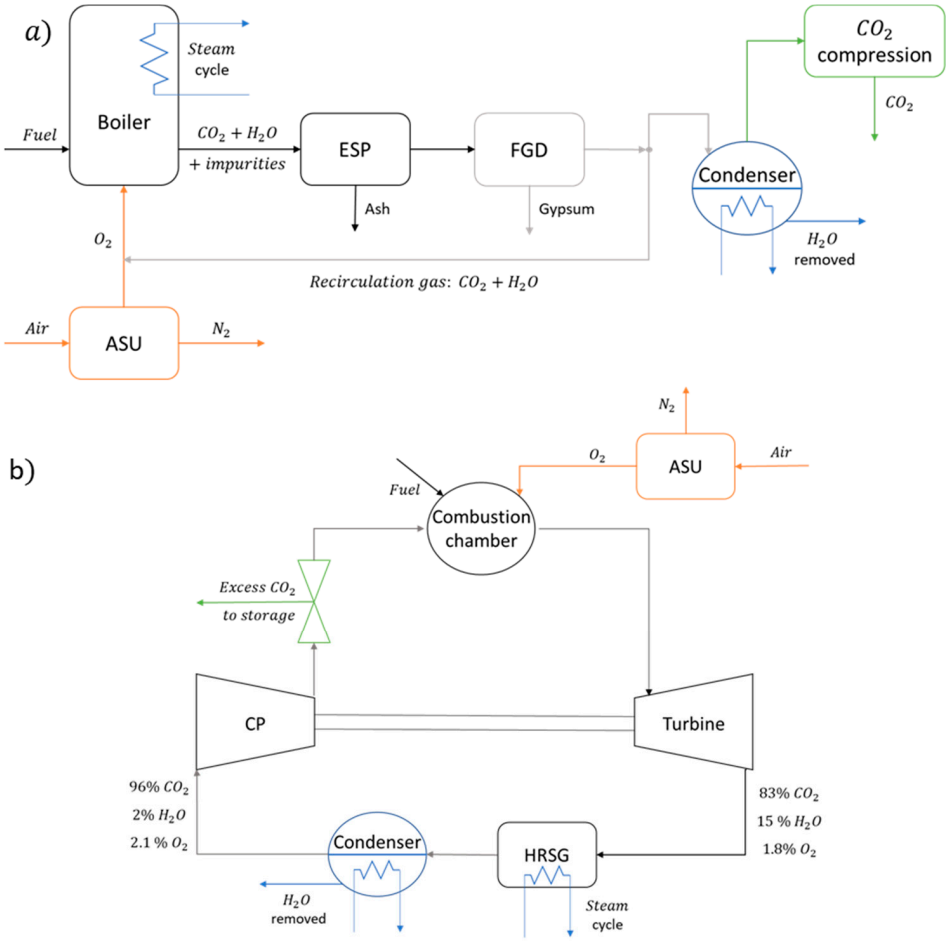

Figure 3. (**a**) Oxyfuel combustion in the Circulating Fluidised Bed (CFB) reactor with CO_2 recirculation coupled with Rankine cycle (secondary cycle); (**b**) gas turbine cycle with CO_2 recirculation (direct cycle). In both plants, the storage receives near pure excess of CO_2 [24].

The flue gas cleaning island is usually composed of an Electro-Static Precipitator (ESP) and a Flue Gas Desulphurisation (FGD) unit. The ESP unit removes the Particulate Matter (PM) in a coal-fired power plant with an efficiency of up to 99.5%. These devices operate at 130–150 °C, but with decreasing emission limits of PM, new low-low temperature ESPs are implemented, operating at 80–90 °C. At this range of temperatures, the electric resistivity of coal dust is lower and the precipitation efficiency can increase (until 99.9%) [25]. In the FGD unit, the flue gas interacts with an absorbing medium producing highly solid slurry. FGDs can be classified as non-regenerable and regenerable processes, depending on the absorbent compound used. Several sorbents are used during this process (e.g., limestone, magnesium lime, seawater and ammonia) and they have different desulphurisation efficiencies [26]. In a gas turbine cycle, the fuel requires a desulphurisation process before the combustion. The purified flue gas flows into a condenser to reduce its water content. Indeed, a dry CO_2 stream is necessary to avoid acid formation. Finally, the temperature and pressure of CO_2 is conditioned depending on the means of transport used (e.g., supercritical condition in the case of pipeline transportation).

Oxy-fuel combustion capture mainly integrates SCPC and USC power plants with low-rank coal (sub-bituminous and lignite). Table 1 shows the range of performance and cost results for new plants. A conventional cryogenic air separator is used for oxygen production, able to produce high quality CO_2 (>99%).

Table 1. Current performance and cost estimates for oxyfuel combustion capture at new (SCPC/USC) plants (values in 2013 US$) [21]. Definition: Higher Heating Value (HHV).

Performance and Cost Measurement for New Oxy-Combustion Plants with Subbituminous or Bituminous Coal			
	Range		
Plant Performance Measurement	**Low**	**High**	**Representative Value**
SCPC/USC reference plant net power output [MW]	550	1030	684
Emission rate w/o capture [t CO_2/MWh]	0.75	0.861	0.83
Emission rate with capture [t CO_2/MWh]	0.017	0.11	0.08
Percentage of CO_2 reduction per MWh [%]	90	98	92
Total CO_2 captured or stored [Mt/y]	3.1	5.5	3.9
Plant efficiency w/o capture, HHV basis [%]	38.7	42	39
Plant efficiency w/capture, HHV basis [%]	30.1	34.1	32
Efficiency penalty [%]	8.1	7.9	8
Capture energy requirement [%more input/MWh]	24	29	25
LCOE w/o capture [$/MWh]	56	68	64
LCOE w/capture [$/MWh]	91	121	110
Increase in LCOE capture only [$/MWh]	35	53	46
Cost of CO_2 captured [$/t CO_2]	36	67	52
Cost of CO_2 avoided [$/t CO_2]	45	73	62

3.2. Pre-Combustion CO_2 Capture

The pre-combustion capture process covers decarbonisation by gasification or steam methane reforming of primary fuel (coal/biomass and methane, respectively), and CO_2 separation. As a result, the plant produces almost pure hydrogen.

The heated primary fuel flows into a gasifier reactor with air (or O_2) and water (or steam), usually pressurised. After the gasification process, the syngas is mainly composed of carbon monoxide, carbon dioxide, hydrogen and methane. At different thermodynamic conditions (pressures and temperatures), the gas composition changes. At high temperatures, the content of methane drops while the percentage of CO increases. Increasing the gasification pressure, the mole fractions of methane and carbon monoxide go up.

The gasification process does not sequester carbon molecules, but it converts carbonaceous solids into a gas product with useful chemical heating value, easily treatable for contaminant removal.

Several configurations can be proposed (e.g., gasifier + Water Gas Shift reactor (WGS) + Solid Oxide Fuel Cell (SOFC)), but the most common technology is the Integrated Gasification Combined Cycle (IGCC). In the plant shown in Figure 4, the hydrogen produced is burnt in a gas turbine to generate electricity, and the exhaust heat from the flue gas lean of CO_2 is recovered to generate steam that drives a steam turbine.

The CO_2 concentration of pre-combustion capture is higher than post-combustion processes, and therefore the energy required for the only CO_2 separation is lower. For IGCC, the CO_2 concentration can be in the range of 35–40%mol after WGS and water removal (15–25%mol if the resource is natural gas [27]) [28]. Table 2 summarized the result of new IGCC power plants with and without a pre-combustion capture system. The physical solvents (e.g., Pressure Swing Absorption (PSA) and Vacuum Pressure Swing Absorption (VPSA)) are the technology mainly used for carbon capture in IGCC plants.

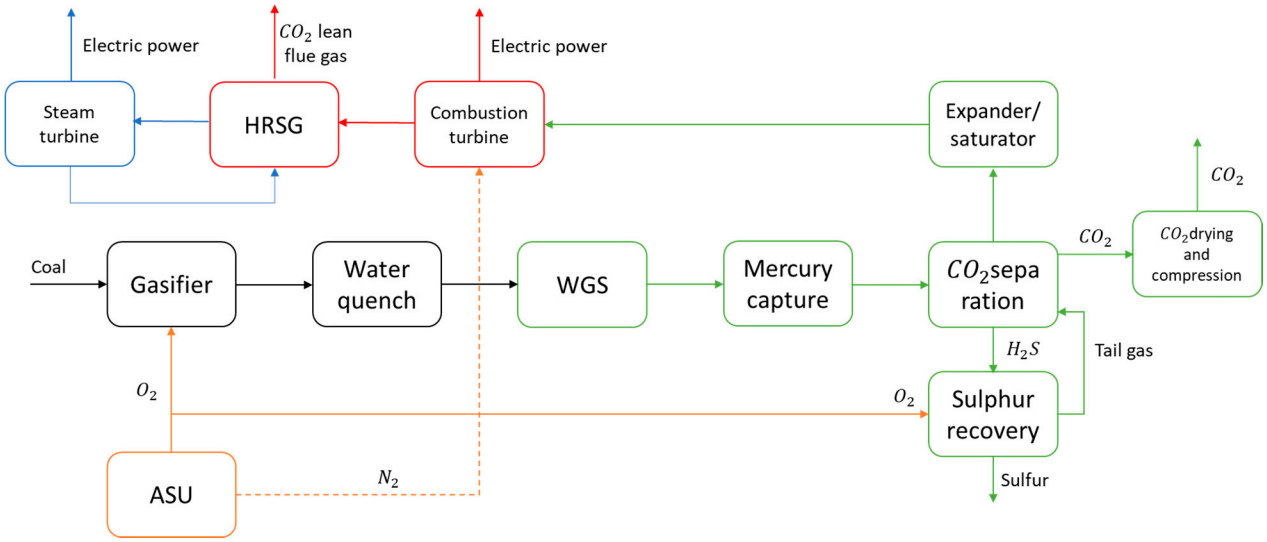

Figure 4. IGCC block flow diagram with CO_2 capture.

Table 2. Summary of the results of new IGCC power plants with and without a pre-combustion capture system [21].

Performance and Cost Measurement for New IGCC Plant with Bituminous or Sub-Bituminous Coal (SCPC)			
	Range		
Plant Performance Measurement	**Low**	**High**	**Representative Value**
SCPC/USC reference plant net power output [MW]	550	1030	753
Emission rate w/o capture [t CO_2/MWh]	0.75	0.84	0.786
Emission rate with capture [t CO_2/MWh]	0.093	0.15	0.104
Percentage of CO_2 reduction per MWh [%]	82	88	87
Total CO_2 captured or stored [Mt/y]	3	6	4
Plant efficiency w/o capture, HHV basis [%]	39	44.2	42
Plant efficiency w/capture, HHV basis [%]	29.9	36.5	33
Efficiency penalty [%]	9.1	7.7	9
Capture energy requirement [%more input/MWh]	21	30	25
LCOE w/o capture [$/MWh]	64	79	69
LCOE w/capture [$/MWh]	100	141	124
Increase in LCOE capture only [$/MWh]	36	62	55
Cost of CO_2 captured [$/t CO_2]	42	87	63
Cost of CO_2 avoided [$/t CO_2]	52	112	81

3.3. Post-Combustion CO_2 Capture

Post-combustion technologies allow the separation of CO_2 from exhaust gases. The CO_2 produced by the combustion of fossil fuels or numerous industrial processes, is purified, concentrated and dispatched to a storage unit. Conceptually, post-combustion capture is the most straightforward technology, and it can be applied in existing plants without substantial changes, only adding the capture process before the flue gases are released into the atmosphere, as illustrated in Figure 5.

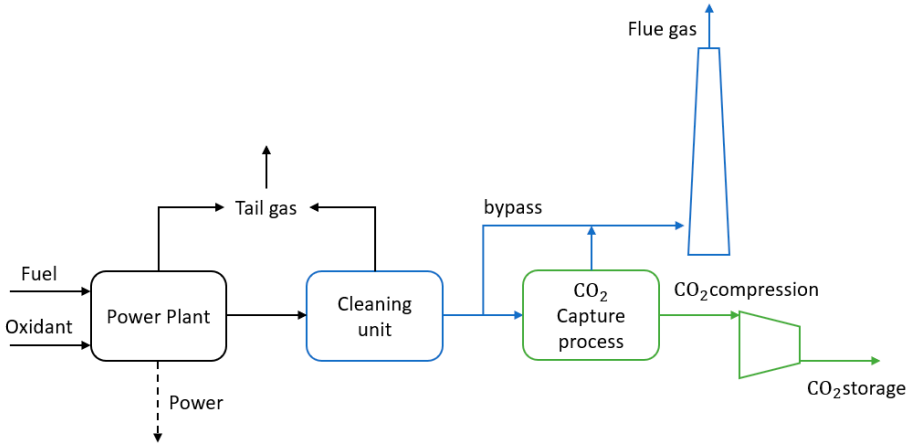

Figure 5. Block flow diagram of power plant with post-combustion CO_2 capture technology.

The mainly post-combustion capture process can be divided into chemical and physical absorption.

The chemical absorption processes are the most used technology for post-combustion capture. They are typically a blend of aqueous amines but can also include amino acid salts, ammonia and ionic liquids, while in the case of solid sorbents they can consist of calcium looping and others.

Liquid absorption processes can treat gas streams with high or low pressure, but the capture rate is affected by thermodynamic conditions. Generally, two stages are sufficient:

1. CO_2 absorption from exhaust gas in an aqueous solution of the solvent in an absorber reactor (low temperatures and high pressures).
2. Solvents regeneration to produce a pure CO_2 stream in a stripper (high temperatures and low pressure).

An optimum solvent has a low regeneration energy demand, high capacity to absorb CO_2, chemical stability, low volatility and limited solvent make-up. The state-of-the-art in solvents is represented by monoethanolamine (MEA), which has acceptably low heat requirements for regeneration, little degradation, and small amine losses. Figure 6 illustrates the block diagram scheme for the absorption/stripper system for CO_2 capture.

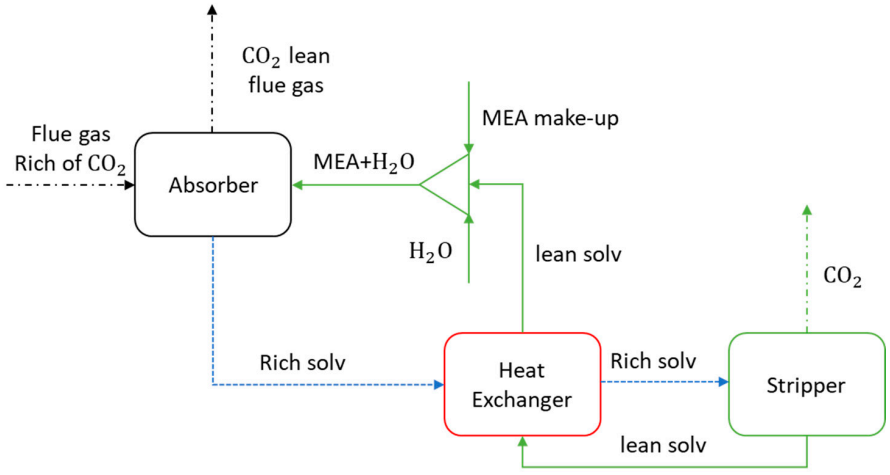

Figure 6. Scheme of post-combustion CO_2 capture with a chemical absorption process using aqueous monoethanolamine (MEA) solution.

The flue gas rich in CO_2 reacts with the MEA in the absorber column producing flue gas lean of CO_2 and carbon-rich amine solution at the bottom of the absorber. The rich solvent is pre-heated in the heat exchanger by the lean solvent regenerated in the stripper.

The rich solvent comes into the stripper, where it reaches 120–140 °C at low pressure in order to regenerate the solution and produce a pure CO_2 stream. The lean solvent supplies its heat to the rich solvent, and it is mixed with make-up MEA and water before entering the absorber column. The primary energy consumption (penalty efficiency) is attributed to the regeneration of the solvent in the stripper column [29].

Table 3 summarizes the results of new SCPC power plants, with and without a post-combustion capture system. The majority of data available for post-combustion capture plants are based on MEA solvents. Several technologies have been developed for post-combustion processes (e.g., Calcium Looping [30,31] and membrane separation [Section 3.4]). Although they offer a future reduction of capture costs, they have not yet been developed for large capture plants.

Table 3. Current performance and cost estimates for post-combustion capture at SCPC power plant (values in 2013$) [21].

Performance and Cost Measurement for New SCPC with Bituminous Coal			
	Range		
Plant Performance Measurement	**Low**	**High**	**Representative Value**
SCPC/USC reference plant net power output [MW]	550	1030	742
Emission rate w/o capture [t CO_2/MWh]	0.746	0.84	0.788
Emission rate with capture [t CO_2/MWh]	0.092	0.12	0.104
Percentage of CO_2 reduction per MWh [%]	86	88	87
Total CO_2 captured or stored [Mt/y]	3.8	5.6	4.6
Plant efficiency w/o capture, HHV basis [%]	39	44.4	41.4
Plant efficiency w/capture, HHV basis [%]	27.2	36.5	31.6
Efficiency penalty [%]	11.8	7.9	9.8
Capture energy requirement [%more input/MWh]	21	44	32
LCOE w/o capture [$/MWh]	61	79	70
LCOE w/capture [$/MWh]	91	130	113
Increase in LCOE capture only [$/MWh]	30	51	43
Cost of CO_2 captured [$/t CO_2]	36	53	46
Cost of CO_2 avoided [$/t CO_2]	45	70	63

The plant with carbon capture requires about 32% of extra energy to reduce the emissions of CO_2 by 87% compared to that without the carbon capture process. MEA technology has a higher Technology Readiness Level (i.e., TRL 9) than other post-combustion capture processes (e.g., chemical looping combustion TRL 6 and membrane polymeric TRL 6) [32].

3.4. Post-Combustion CO_2 Capture with Membrane Technology

Recently, an increased interest in gas separation for hydrogen production, air separation, biogas upgrading, and CO_2 sequestration from flue gas has been observed. Membrane-based gas separation technology can be used for the above aims. Membranes are produced as a thick film able to separate a mix of gases when there are driven forces (pressure and molar gradients).

The permeate is the gas separated from the mixture able to pass through the membrane to the low-pressure environment while the retentate is the remaining part of the original mix. Figure 7 shows the basic arrangement of this type of separation process.

Concerning the CO_2 separation process, membrane technology is used to upgrade biogas, increasing methane content in Natural Gas (NG) or Synthetic Natural Gas (SNG), reaching the purity established by the gas network, or as post-combustion capture to sequestrate the CO_2 from fuel combustion.

The membrane process shows several advantages compared to the other CO_2 separation technologies: (i) no regeneration process; (ii) design without moving components; (iii) lower maintenance; (iv) high reliability [33]. On the contrary, the main drawbacks are higher energy requirements and as yet no process at a massive scale.

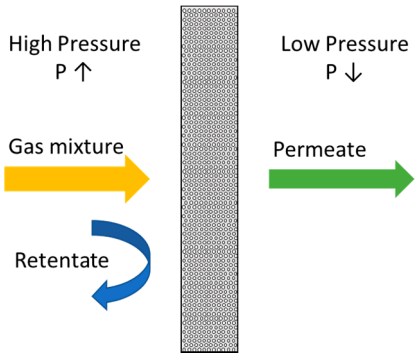

Figure 7. Gas mixture separation with membrane films. Only part of the gas mixture permeates through the membrane, passing from the high pressure to the low-pressure side.

Low production costs, high gradient pressure, excellent work at the no-stress environment, and the possibility to scale-up are the main benefits of polymeric membranes, which are used mainly for gas separation despite their limited robustness, aging and swelling problems. The gas moves through the pores of the polymeric membranes. The primary mechanism of the gas separation process is dissolution on the feed side and diffusion across the membrane.

Polymeric membranes account for the main share of the global gas separation membranes market (77.46% in 2015) [34]. Nevertheless, inorganic membranes will certainly play an essential role in gas separation processes due to their significantly longer lifetime and lower environmental impacts. Inorganic membranes can be made of ceramic, metal, and carbon material and, in some cases, by a mixture of these materials. The different separating or transport mechanism depends on whether the microstructure of the membrane is dense or porous. The primary membranes for gas separation are dense ceramic membranes, dense metallic membranes, and microporous membranes.

Mixed Matrix Membranes (MMMs) consist of a continuous polymeric matrix in which nanoparticles of inorganic materials are immersed. They are considered new generation membranes for gas separation, combining the characteristics of polymer and mineral fillers. The incorporated inorganic material, such as zeolites, silica particles and Metal-Organic Framework (MOF), is added to improve the properties of the polymers [35].

The performance indicators depend on the dominant mechanism of gas permeation through the membrane. Nevertheless, permeability and selectivity are common for evaluating membrane separation, and they are the main performance indicators.

Permeance is the most common parameter used in the membrane industry, and it is defined as the rate at which gas moves through the membrane under a standard pressure driving force. It is frequently measured as a Gas Permeation Unit $GPU = 10^{-6}\ \mathrm{cm}^3_{\mathrm{STP}}/\left(\mathrm{cm}^2\mathrm{scmHg}\right)$. Instead, the permeability is the permeance multiplied by membrane thickness, and it shows the intrinsic property of the gas to pass through the membrane and corresponds to the productivity of the membrane separation stage. It is also measured in $barrer = 10^{-10}\ \left(\mathrm{cm}^3_{\mathrm{STP}}\mathrm{cm}\right)/\left(\mathrm{cm}^2\mathrm{scmHg}\right)$.

The ability of a membrane to separate a target gaseous component from a mixture of two gases (i and j) is called selectivity or separation factor. It is an essential feature for separation applications, and it represents the efficiency of the membrane separation stage. Selectivity is measured by considering the molar fraction of single component on the permeate (y) side over that on the feed (x) side:

$$\alpha_{i,j} = \frac{y_i/y_j}{x_i/x_j} \tag{7}$$

The PolarisTM membranes developed by the Membrane and Technology Research Institute (MTR) [22] overcome the main challenge of post-combustion capture. Indeed, the low partial pressure of flue gas leads to a huge membrane area. PolarisTM membranes have

ten times the permeance of conventional gas separation membranes and, together with a new sweep module for the selective recycling of CO_2, drive efficient overall CO_2 recovery up to 90%. The main goal of MTR was to increase membrane permeance to decrease the required membrane area and reduce the capital cost of the membrane CO_2 capture system. The first membrane developed had CO_2 permeance of 1000 GPU and CO_2/N_2 selectivity of 50. Over time, the membrane performance has improved to 1700 GPU for second-generation (commercial scale) and almost 3000 GPU for the third one (only in lab-scale).

A new design for a small pilot membrane system was installed at the National Carbon Capture Center in July 2014. Several test campaigns have confirmed its efficient capacity to capture CO_2 achieving 90% CO_2 capture, while the very simplicity and tiny size of this technology gives it an advantage with respect to the other capture systems. The new configuration illustrated in Figure 8 was sized to treat 20 t CO_2/day included in flue gas at 11% of CO_2 and 50 °C, improving the TRL from 3 (lab scale) to 6 (pilot plant).

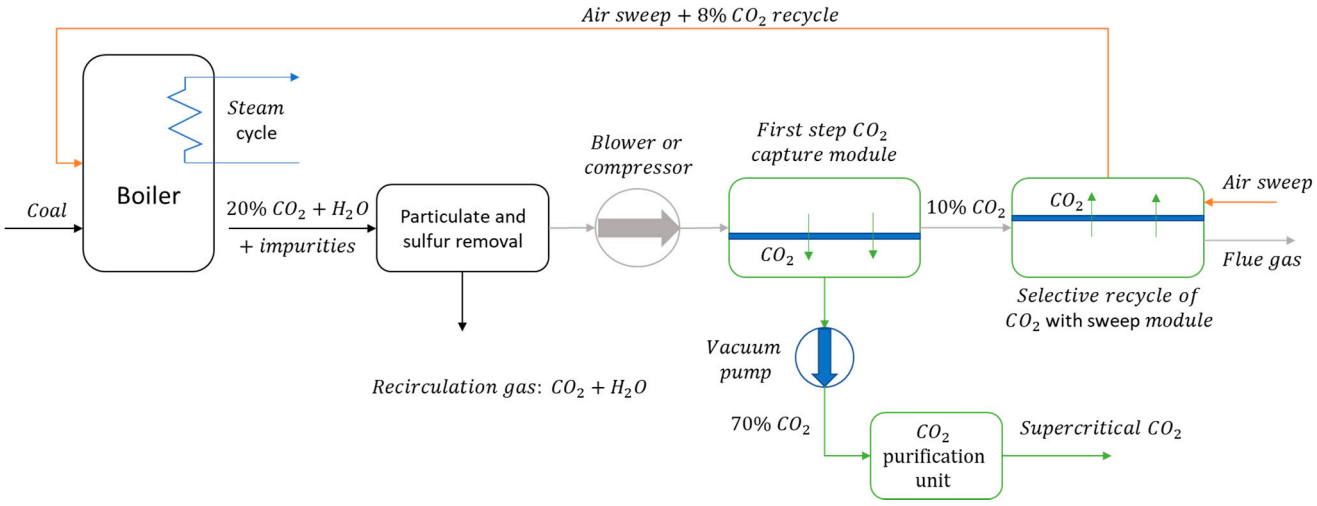

Figure 8. Simplified diagram of the Membrane and Technology Research Institute (MTR) selective recycle CO_2 capture process at a coal-fired power plant using PolarisTM membrane in separation modules [22].

The membrane separation process designed by MTR/DOE and illustrated above is equipped with a multi-stage membrane treatment. The flue gas produced in a boiler flows into a cleaning unit in order to remove contaminants, and then it is pressurized. The pressurized flue gas flows into the first step CO_2 capture module. The driven force used to separate the CO_2 is mainly the gradient pressure obtained by means of a compressor on the feed side and a vacuum pump on the permeate side. In this first module, only part of the CO_2 is separated from the flue gas. The remaining carbon dioxide in the depleted flue gas is sequestrated via the second sweep module. This component uses air combustion as a sweep stream to generate a driving force and therefore compressors and vacuum pumps are not used. The CO_2 permeates the membrane to produce a diluted air combustion. As a result, the flue gas produced in the boiler has a higher CO_2 concentration (i.e., ≈20%). With the configuration described above, the separation efficiency of the first module increases (about 90% of CO_2 is captured) producing a rich mixture gas composed mainly of 71% of CO_2, 9% of H_2O and 18% of N_2, which is sent to the CO_2 purification unit.

The techno-economic analysis was performed integrating a supercritical coal power plant delivering 550 MWe with the new membrane technology of MTR, and it is summarized in the following Table 4.

Table 4. Techno-economic analysis for CO_2 separation with membrane technology performed by MTR for post-combustion capture in SCPC coal-fired power plant [22].

Performance and Cost Measurement for New SCPC with Bituminous Coal Integrated with the Membrane Capture System	
Plant Performance Measurement	**Representative Value**
SCPC/USC reference plant net power output [MW]	550
Emission rate w/o capture [t CO_2/MWh]	0.788
Emission rate with capture [t CO_2/MWh]	0.111
Percentage of CO_2 reduction per MWh [%]	89.9
Total CO_2 captured or stored [Mt/y]	4.8
Plant efficiency w/o capture, HHV basis [%]	39.3
Plant efficiency w/capture, HHV basis [%]	28.6
Efficiency penalty [%]	10.7
LCOE w/o capture [$/MWh]	76.9
LCOE w/capture [$/MWh]	120.4
Increase in LCOE capture only [$/MWh]	43.5
Cost of CO_2 captured [$/t CO_2]	44
Cost of CO_2 avoided [$/t CO_2]	64

4. Large-Scale Transport of CO_2

CO_2 can be transported in the solid, liquid, or gas phase. Liquid phase transportation is a critical method due to topographic variations that could cause pressure drop and temperature change, which leads to two-phase flow liquid-gas. Therefore, the most efficient way to transport CO_2 is in the supercritical phase (pressure higher than 7.38 MPa and temperature of more than 31.2 °C). The transportation via pipeline is characterized by a steady-state supply of CO_2 without temporary storage, while ship transport becomes feasible for long distances or overseas.

CO_2 has been transported by pipeline for many years to industry users (e.g., food production, winemaking, oil recovery) while, in recent years, millions of tonnes of CO_2 have been transported to the USA and Canada for EOR. Therefore, it is a mature technology, though a significant effort would be required to scale up the infrastructure to manage the global captured target of 7 Gt/y [36], which is much larger than the approximately 50 Mt/y transported for EOR in the USA [37].

4.1. CO_2 Thermophysical Properties

The transportation chain starts from the conditioning of a CO_2 rich stream from a capture process and ends with the injection into the storage sink. Between these two points, the CO_2 transportation can take place via pipeline, ship or tanker trucks. Pipelines today operate as a mature market technology. The CO_2 gathered from different capture technologies from sizeable stationary emission sources (e.g., industries and power plants) is conditioned, to remove impurities, and typically compressed up to 80 bar to avoid two-phase (i.e., liquid-gas phases) flow regimes and density increase. When it is transported via ship or road or rail tankers, the liquid CO_2 carried is insulated at a low temperature and pressure in tanks. Usually, the thermodynamic designs for semi-refrigerant tank types are −54 °C and 6 bar or −50 °C and 7 bar [38].

CO_2 can be transported in all three phases. For example, during pipeline transportation, pressure drops and temperature changes can cause a phase change. Therefore, it is crucial to know the CO_2 phase diagram reported in Figure 9a. The phase diagram contains two important points: (i) triple point (−56.6 °C, 5.2 bar), the three phases of the substance coexist in thermodynamic equilibrium; (ii) critical point (31.1 °C, 73.8 bar), above which the substance exists as a supercritical fluid. In this last phase, CO_2 has the density of a liquid and viscosity of a gas [39].

After purification, CO_2 is dried to remove water particles and avoid corrosion to carbon and low-alloy steel lines. Indeed, moisture condensation can cause carbonic acid

formation. After this process, the CO_2 is pressurized to often achieve a dense phase fluid, increasing pipeline transportation efficiency.

The behavior of the captured CO_2 depends on its composition. The composition relies upon the source type (e.g., power plant, industrial process), capture technology (e.g., post-combustion, oxy-combustion, pre-combustion), and fuel type. It may contain other chemical species like water vapour, CH_4, N_2, H_2S, O_2, and several other hydrocarbons. The presence of impurities has a significant impact on the physical properties (phase diagram) and hydraulic parameters (e.g., density, viscosity), as illustrated in Figure 9b. Therefore, a CO_2-rich mixture diagram is necessary to design the transportation correctly.

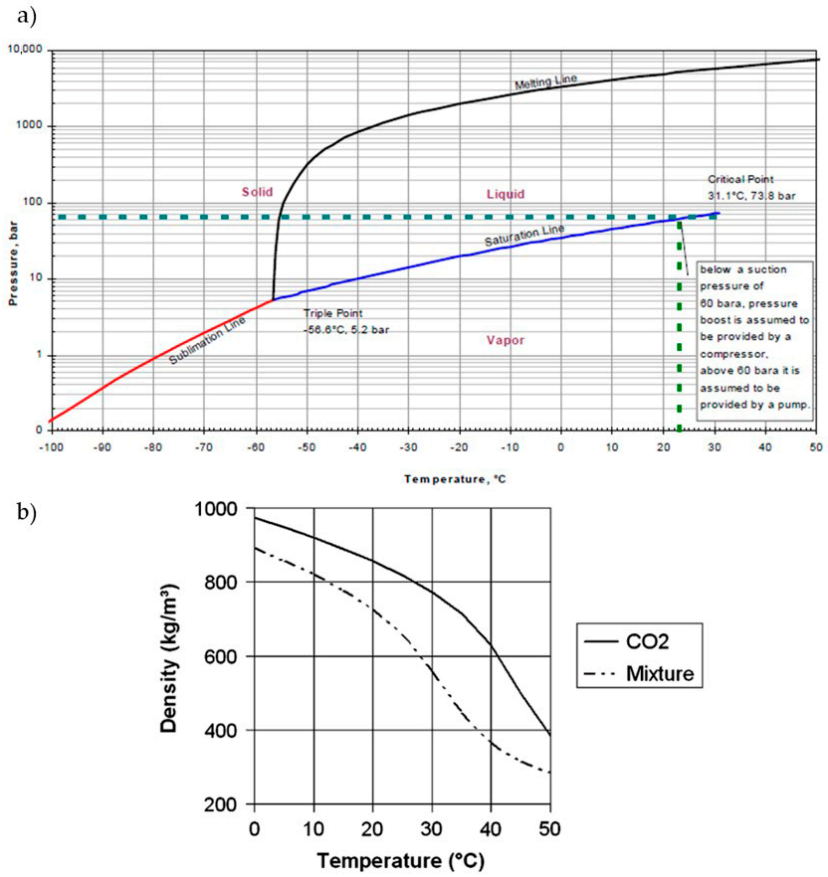

Figure 9. (**a**) CO_2 phase diagram; (**b**) difference in density of pure CO_2 and CO_2 rich mixture [95% CO_2/3% N_2/2% O_2] at 100 bar. International Energy Agency (IEA) [Woodhill] (2002) Pipeline transmission of CO_2 and energy transmission study-report. All rights reserved [39].

This alteration has both technical and economic implications. The pumped system is recommended to keep the CO_2 under the supercritical phase all along the pipeline. Further attention has to be paid to the depth variation, which induces temperature and pressure change.

It has been highlighted that the presence of free water in the CO_2 stream should be avoided, and its content should be limited between 50–600 ppm [40]. The level of moisture depends on the quantity of SOx, NOx, and H_2S contained in the CO_2 stream, which can be formed in the presence of aqueous phase sulphuric and nitric acids and cause a pH drop of the solution. Therefore, the gas purification steps are essential to adjust the composition and obtain high CO_2 concentration.

4.2. Economic Evaluation of CO_2 Pipeline Transportation

Several works explain different cost models for pipeline transportation, but all of them give inconsistent results [41] due to different topographic conditions (e.g., onshore vs.

offshore), geographical regions, which influence labour, and the right to travel under or over private land (Right-Of-Way cost (ROW)), assumption (e.g., lifetime, capacity factor), material (e.g., steel, coating, insulation), incorporated costs (e.g., initial pressure).

The transport cost model developed by the National Energy Technology Laboratory (NETL) [42] estimates the cost of transporting dense phase CO_2 using a single point-to-point pipeline. The model has a level of accuracy between +50/−30%, and the analysis includes:

- Capital costs: Purchasing and installing the pipeline, surge tank, control system, and booster pump.
- Operation and Maintenance costs: For pipe, pump, and electricity to power pumps.

The costs of the material and installation of the pipeline depending on the diameter and length of the pipe.

The diameter is a function of CO_2 mass flow rate, pressure losses due to elevation difference and rugosity of the material, and the number of boost pumps. The CO_2 stream is assumed to be pure for the sake of simplicity.

Every segment of the pipeline is divided by pump stations and has the same length, inlet pressures equal to the initial inlet pressure, and outlet pressures identical to the end outlet pressure for each segment, while in the case of elevation difference, all the branches of the pipeline have the same variation. In this way, each pipe has the same pressure loss and elevation changes.

The transport cost model provides three methods for inner diameter calculation:

1. McCollum and Ogden.
2. Heddle et al. and MIT.
3. McCoy and Rubin.

As a result, the inner diameter obtained in the three methods is rounded up to the near-standard diameter.

The transport cost model computes the capital cost, which is incurred only during the project construction years, and operating cost, which is incurred during the project operation years.

Detailed construction costs for CO_2 pipelines are not available, and for this reason the capital cost model is based on the natural gas pipeline data set, and the numbers provided are assumed as the as-built-cost. The capital cost of the pipeline can be divided into four categories: (i) materials: pipe, coating and cathodic protection; (ii) labour costs; (iii) ROW and damage; and (iv) miscellaneous: engineering costs, supervision, contingencies, telecommunication equipment, taxes, administration and overheads, and regulatory filing fees.

Three equations provided by Parker [43], McCoy and Rubin [44], and Rui et al. [45] are taken into consideration to compute the capital cost of the pipeline,

Finding these values, the model changes them to CO_2 pipeline costs through several different coefficients, depending on the equation chosen.

The following Table 5 summarises the main input parameter used in the analysis.

Figure 10a demonstrates that the method used to calculate the inside diameter of the pipeline did not affect the final result. In contrast, the three methods utilized to compute firstly the capital cost of the natural gas pipeline and then the CO_2 pipeline, illustrated in Figure 10b, give significantly different results.

The Parker equation always gives the highest cost compared to the others, while the estimation cost of CO_2 transportation using the Rubin method is lower. Rui and Rubin's methods show a slightly decreasing trend with the increasing length of the pipeline; on the contrary, the Parker method does not describe cost reduction as the length of the pipe goes up. The analysis was obtained through an iterative calculation of the inner diameter, pressure drops, and several other parameters. The transportation cost also includes the optimal number of pumps used to avoid CO_2 phase change.

Table 5. Financial parameters and technical parameters used to perform an economic analysis of CO_2 transportation.

Financial Parameters	
Capitalization	50%
Cost of Equity	12%
Cost of Debt	4.5%
Tax Rate	24%
Escalation Rate	3%
Project Contingency Factor	15%
Depreciation method-recovery period for depreciation	DB150—15 years
Duration of Construction in years	3
Duration of Operation in years	30
Technical Parameters	
Annual tonnes of CO_2 Transported (on average) [Mt/y]	5
Capacity Factor	80%
Inlet Pressure [MPa]	15.3
Outlet Pressure [MPa]	8.4
Change in elevation [m]	0
Temperature of the environment [°C]	12
Pump efficiency	75%

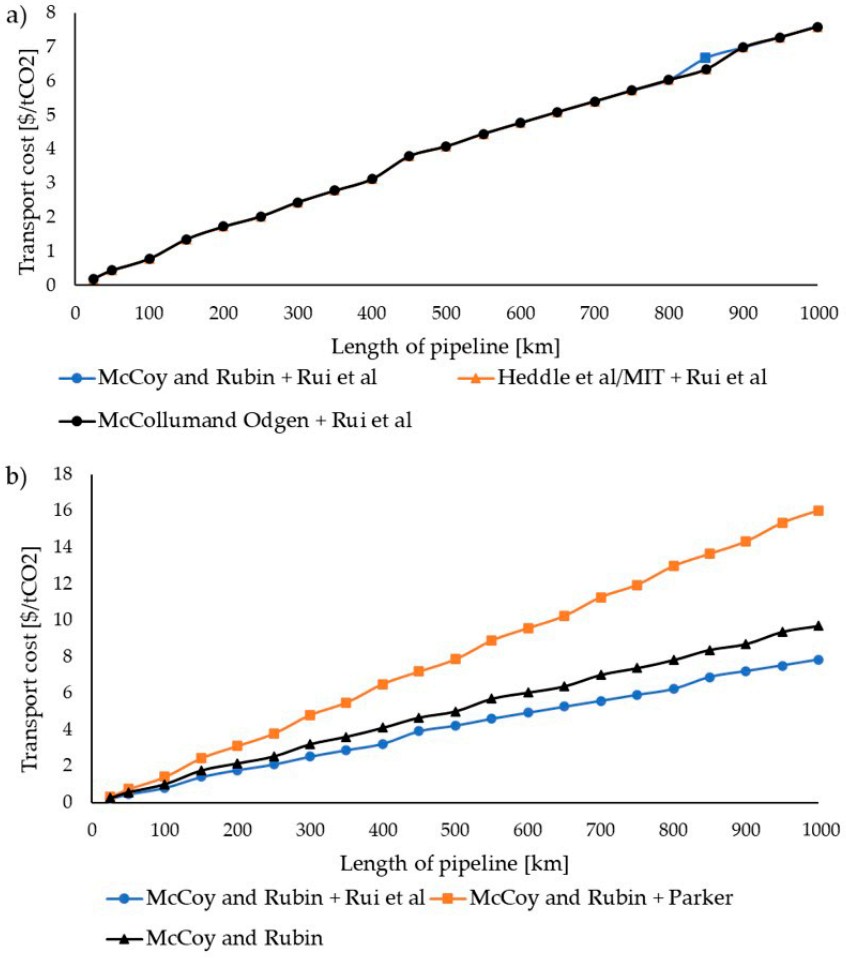

Figure 10. CO_2 transport cost computed with 2013 in dollars. (**a**) To obtain this graph, three different methods are used to calculate the inner diameter while the same method (Rui et al.) is used for the economic analysis. (**b**) In this graph, we used the same method (McCoy and Rubin) to compute the inner diameter, while various ways are used to carry out the economic analysis.

5. CO_2 Sequestration and NGH Purification

Storage of carbon dioxide from a power station or industrial facilities can be feasibly done as climate change mitigation options in subsurface formation within or below the ocean or under the ground. Considering the large-scale capture and storage, it is crucial to highlights the toxicity of CO_2. The concentration in the atmosphere is around 0.04% but, if it increases up to 10%, the CO_2 acts as an asphyxiant while, if it rises until 20%, the inhalation leads to rapid death. Therefore, once stored, the site will need to be monitored for many years to verify that CO_2 can never be released to the atmosphere.

The main types of underground storage site are:

- Oil and gas wells. They are immediately accessible and used for EOR. During the extraction process, it is possible to achieve an oil with high viscosity (i.e., heavy oil) that it is impossible to extract with conventional methods. The injection of CO_2 is one method to enhance oil recovery. The gas remains underground after pumped while the oil can be extract. The sequestered CO_2 have to be monitored every days [46]. It can also be used depleted oil and gas fields, providing a storage capacity that will often have pipeline access but with limited capacity.
- Coal beds too deep to be mined. These coal beds (relatively rare) usually contain methane, and therefore carbon dioxide can replace it. The recovery methane will offset the cost of carbon dioxide sequestration.
- Brine aquifer. It is created when a cap of impermeable rock is formed deep underground and prevents water and gas seeping upwards. It can potentially be the most critical type of underground site in which CO_2 can replace the brine to remain securely stored.
- Sequestrating CO_2 as hydrate. Potentially, the CO_2 can be trapped as clathrate hydrates into deep oceanic basins, depleted or existing natural gas hydrate reservoir, sub permafrost region with unfrozen water, and depleted oil and gas partially saturated with water.

5.1. CO_2 Storage as Clathrate Hydrates

Subsurface CO_2 permanent sequestration through clathrate hydrates formation is a novel method to mitigate global warming. Gas hydrate are clathrate compounds in which some guest gas molecules (e.g., CO_2, CH_4, C_2H_6) are encapsulated in water molecules. The gas hydrate form under low temperature and high-pressure conditions via hydrogen bonding between water molecules. Reserves of methane in hydrate structure are abundant in geological accumulations in offshore and permafrost environments, and they exceed the all-carbon fossil fuel [47].

Three methods are used to shift the equilibrium and produce methane from oceanic sediments: (i) thermal stimulation through direct heating or injection of heated fluid; (ii) depressurization is the preferred technique for driving gas hydrate dissociation; (iii) injection of chemical inhibitors; (iv) gas swapping [48]. The thermal stimulation method requires a continuous energy source to raise the hydrate temperature above the stability point. The depressurization method decreases the hydrate pressure under the stability point, causing hydrate dissociation. Inhibitor injection involves the injection of a compound at isobaric conditions that shift the equilibrium point to the lower temperature. The injection of CO_2 molecule into NGH deposits involves the replacement of CH_4 into the water cages that leads to produce methane and store carbon dioxide.

CO_2 forms a stable hydrate structure at lower pressure conditions than CH_4 hydrates at the same temperature, as it is showed in Figure 11. Therefore, CO_2 hydrates are more stable than CH_4 hydrates under certain conditions (i.e., CO_2 and CH_4 hydrates equilibrium curves intersect at around 10.5 °C and 75 bar), and it can displace the methane in the hydrate structure. In this way, it enables low carbon energy recovery (e.g., CH_4) while offsetting capture and transportation cost. Besides, CO_2 can re-occupy the pore space from methane recovery, maintaining the mechanical stability of the rock and preventing possible hazards of slope failures. Uchida et al. [49] have demonstrated via experiment and

theoretical calculation that, at a temperature below 10 °C, the equilibrium pressures of the CO_2 hydrates are lower than those of CH_4 hydrate.

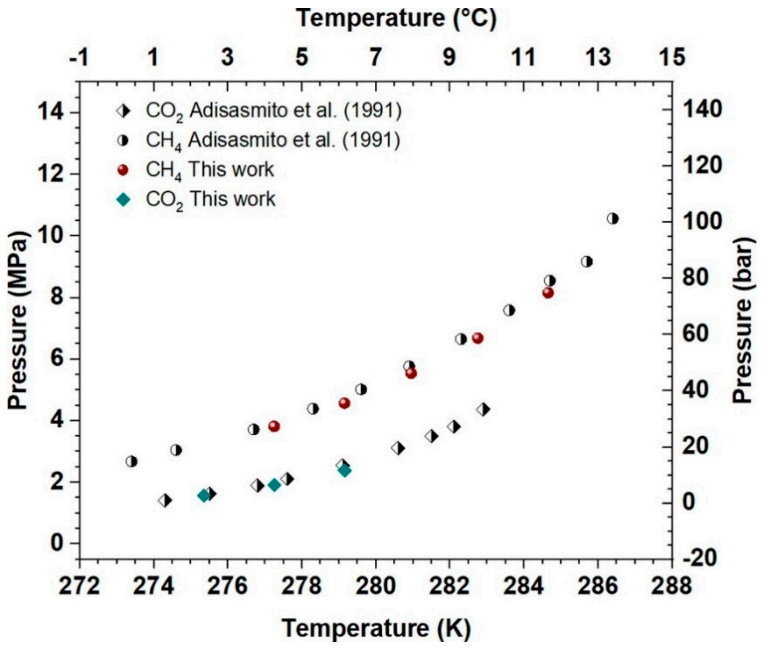

Figure 11. Phase diagram (equilibrium temperature as a function of pressure) for pure CO_2 and pure CH_4 gas hydrates [50]. Reprinted from Applied Energy, Vol 280/edition number 115,843, Quang-DuLe et al. Influence of the initial CH4-hydrate system properties on CO_2 capture kinetics, Copyright (2020), with permission from Elsevier.

CO_2 and CH_4 molecules form both the type SI of crystal-structure hydrate that consists of six medium cages and two small cages. During the hydrate formation, the CO_2 molecule, which is slightly larger than the CH_4 molecule, only occupies the medium cages, while the methane molecule occupies both medium and small cages. As a result, more CH_4 can form in the early stages. The heat of CO_2 hydrate formation (-57.9 kJ/mol) is greater than the heat of dissociation of CH_4 hydrates (54.5 kJ/mol). Therefore, a replacement reaction occurs in the later stages due to the favorable exothermic process [51]. The exothermic nature of the CO_2 hydrates formation provides the heat of methane dissociation and increases the storage temperature. Therefore, the storage's temperature is a critical parameter that has to remain below 10.5 °C to avoid CO_2 dissociation and CH_4 hydrate re-formation.

Lee et al. have examined CH4 and CO_2 molecule distribution over the two cage sites (i.e., S and M) by Magic Angle Spinning Carbon-13 Nuclear Magnetic Resonance (MAS ^{13}C NMR) into a hydrated sample. This analysis shows a limit to the CO_2 replacement degree. It was estimated that 64% of methane can be recoverable from the NGH reservoir, resulting, after only via the exchange of CO_2, a product hydrate with a CO_2/CH_4 ratio of 1.8 or greater at equilibrium condition. Otherwise, a kinetic test showed that the replacement reaction is almost complete in less than five hours, and the product hydrate results with a CO_2/CH_4 ratio of 1. Consequently, 50% of methane included in the reservoir can be replaced by CO_2, and therefore a complete methane recovery is not possible [52].

The mixture of carbon dioxide and methane gas is present in the hydrate reservoir when the CO_2 is injected into the NGH. Adisasmito et al. proposed the following polynomial equation fitted to the experimental data to measure the gas mixture's equilibrium condition in hydrate form [53].

$$\ln(P_{eq}) = 175.3 - \frac{89009}{\mathrm{T}} + 0.07392 \times y + \frac{1.1307 \times 10^7}{T^2} - \frac{23.392 \times y}{T} + 3.9566 \times 10^{-5} \times y^2 \quad (8)$$

The equilibrium pressure P_{eq} is measured in MPa, the temperature T is in °K, and y is the mole percent of carbon dioxide in the vapor phase. The above equation was fitted for a temperature between 273 K and 288 K, while the maximum pressure of the CO_2 was selected not to exceed 4.37 MPa to avoid the formation of liquid CO_2. Indeed, at a pressure higher than 4.37 MPa, the dissociation of methane hydrate occurs at a higher temperature than the hydrate formation of liquid CO_2. Therefore, at high pressure, the CO_2 might not sequester as hydrate and can cause instability of the seafloor. The equilibrium condition of the hydrate mixtures is shown in Figure 12.

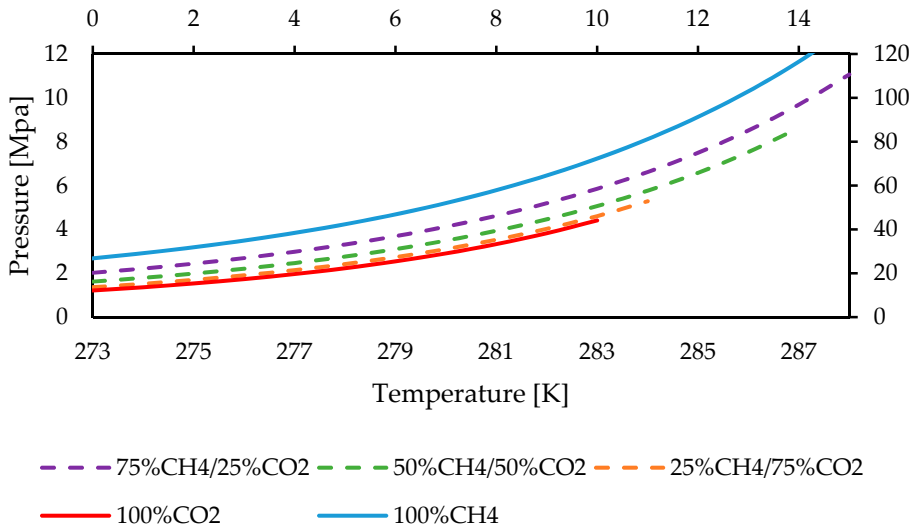

Figure 12. Hydrate phase equilibrium of a mixture of carbon dioxide and methane from Equation (8).

The upper and lower limit of the phase equilibrium diagram represents the cases of pure methane and pure carbon dioxide hydrates, respectively. The equilibrium conditions for the mixed gases lie between these two limits. The figure shows that at a fixed temperature, the equilibrium conditions move to lower pressure and, at a fixed pressure, they move to a higher temperature when the CO_2 mole fraction in the mixture increases.

The experiments above are conducted in the bulk phase; however, the dissociation of methane hydrate and its replacement via carbon dioxide occur in sediment reservoirs. Therefore, this process needs to be studied in porous media. Figure 13 compares the hydrates equilibrium conditions in porous media with those in the bulk phase [54].

The experimental data are measured mainly in porous silica gel and porous glass, and they are represented via symbols, while the lines represent value obtained by correlations. The figure shows that the equilibrium pressure is higher at a temperature while, at a pressure, the equilibrium temperature is lower in porous media than in the bulk phase. Besides, from the last two figures, we can deduce that increasing the CO_2 mole fraction in the hydrate deposits will reduce the favorable range of temperature and pressure. Consequently, an accurate range selection is needed for simultaneous methane production and carbon dioxide sequestration [54].

The processes of hydrate formation and dissociation in porous media are different to respect those in the bulk phase. In porous media, the hydrate will first form in the smaller size pores as the temperature decrease. On the other hand, if the temperature increases, the hydrates will first dissociate in the largest pore. The injected CO_2 can form hydrate into a pore throat blocking the pore. As a result, the hydrate particles can isolate large quantities of methane hydrate in a deeper pore and hampers further methane dissociation and carbon dioxide sequestration. Clennest et al. have predicted the hysteresis cycle between crystallization temperature and the dissociation of the clathrates in porous media [55]. Concerning the heat of dissociation and formation of the hydrates, several researchers have yielded conflicting results and therefore need further investigation [54].

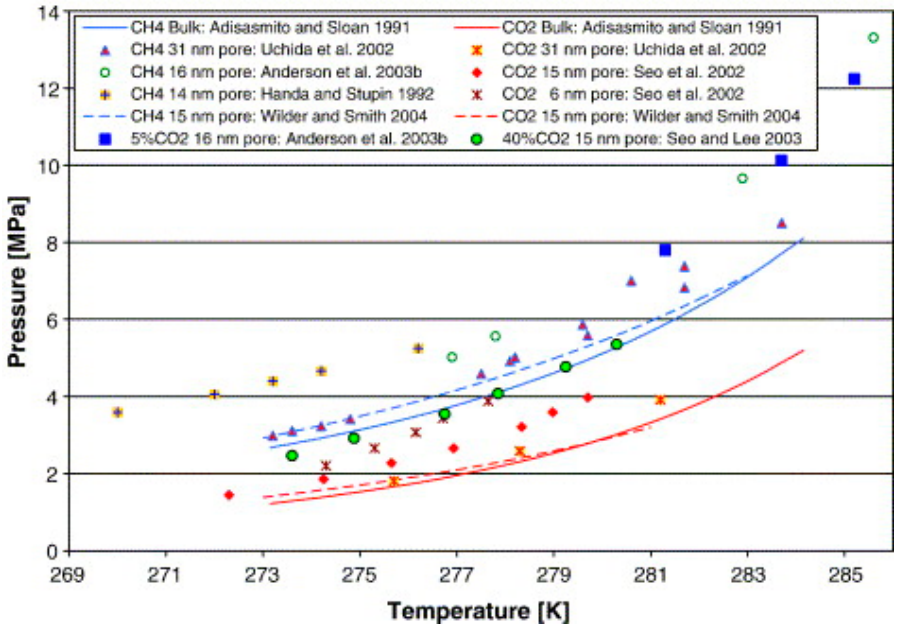

Figure 13. Equilibrium condition for methane and carbon dioxide hydrate in porous media and in bulk phase reprinted from [54] with permission from Elsevier.

Gambelli et al. have tested the CO_2 replacement into NGH deposit via a combination of two strategies. Once the CH_4 hydrate formation is carried out, the replacement phase is performed via depressurization and CO_2 injection. The quantity of CO_2 stored depends on the sum of two contributions: the methane replacement and an ex-novo CO_2 hydrate formation. The CO_2-CH_4 exchange in methane hydrates is favorable; however, the new CO_2 hydrate formation around and the superficial replacement process limit the transition of the CO_2 into the deeper layer inside the deposits and, therefore, the overall replacement process. As a result, the storage efficiency (i.e., the ratio between the moles of CO_2 permanently stored into the NGH and the total amount of CO_2 injected inside the deposit) is limited at 36% with a value of sand pore saturation degree equal to 7.6% [56].

$$\eta_{\text{storage}} = \frac{n_{CO_2\ stored}}{n_{CO_2\ injected}} \tag{9}$$

An experimental apparatus able to promote methane production via a combined CO_2 replacement and depressurization was tested by Zhao et al. [57]. In this manuscript, they run two tests conducted with and without depressurization combined replacement method. This experiment shows the great benefit of the combined method, increasing methane replacement from 7% without depressurization to 25% with a mixed method [57].

Japan and China have carried out methane production testing in oceanic NGH reservoir, showing the possibility and feasibility of methane production by depressurization. Four tests are conducted, three in Nankai Trough (Japan), and one in Shenhu Area, China. The first Japanese test was done in March 2013, but the methane production was interrupted only after six days due to the abrupt sand production. The other two tests were performed in the same location in 2017 but also, in this case, the trials lasted 12 and 24 days, respectively. China has extracted from an oceanic NGH reservoir via a single vertical well by depressurisation method in the same period. China's test was performed in the South China Sea for 60 days. The average daily gas production rate falls between 2.9×10^3–8.3×10^3 in both test sites, with a peak of 2×10^4 m^3/day [58].

5.2. Carbon Dioxide Replacement Cost and Conventional Storage Cost

The recovery of methane from NGH and its replacement with CO_2 molecule remains very challenging, and no previous work on the open literature have reported its cost.

Only a few studies have commented on the economics of methane production from NGH reservoirs, and one of these is used to extrapolate the infrastructure's data cost. In fact, Vedachalam et al. [59] have analysed the techno-economic methane production based on the depressurization method. This method involves a vertical well that connects the NGH formation with a Floating Production Unit (FPU) with a pump able to depressurize the reservoir. The main cost parameters are summarized in the Table 6 below:

Table 6. Cost data used to compute the simultaneous CO_2 storage and methane production.

Cost Element	Unit	Number of Wells			
CAPEX		1	2	5	10
Mob & Demob	[$\$ \cdot 10^6$]	1.5	1.5	2	2
Top Side System	[$\$ \cdot 10^6$]	250	250	350	350
Subsea system	[$\$ \cdot 10^6$]	5	10	25	50
Drilling & Completion	[$\$ \cdot 10^6$]	1.5	3	7.5	15
OPEX	[$\$ \cdot 10^6$/year]	2	4	10	20

We have assumed that the cost data summarized in Table 6 for methane production via depressurization method are the same when a combined method (i.e., CO_2 replacement + depressurization) is applied. The main financial and technical parameters used as input in this simulation are summarized in Table 7. The lifetime of the plant is set up at 15 years [58]. We have assumed that the CO_2 only replaces methane hydrate and does not form a new hydrate to facilitate the economic simulation.

Table 7. The financial and technical parameter to evaluate the CO_2 storage cost.

Financial Parameters	
Capitalization	50%
Cost of Equity	12%
Cost of Debt	4.5%
Tax Rate	24%
Escalation Rate	3%
Project Contingency Factor	15%
Depreciation method-recovery period for depreciation	DB150—15 years
Duration of Construction in years	3
Duration of Operation in years	15
Technical Parameters	
Annual methane production [Mm^3/y/well]	3
Capacity Factor	80%
Price of methane in japan (2019) [$\$/m^3$] [60]	0.335
$\eta_{storage}$ [56]	36%
Annual CO_2 stored [Mm^3/y/well]	3

The tests defined the annual methane production performed both in Japan and China sites, and it was assumed that could be the same when the combined method is applied. The syngas produced from NGH is not composed only of methane but also the injected CO_2 that does not participate in the reaction [56]. As a result, the produced syngas comprises 36% CH_4-66% CO_2 at the chosen storage efficiency. The economic analysis was conducted for different numbers of wells, and the minimum cost to store one ton of CO_2 is illustrated in Figure 14.

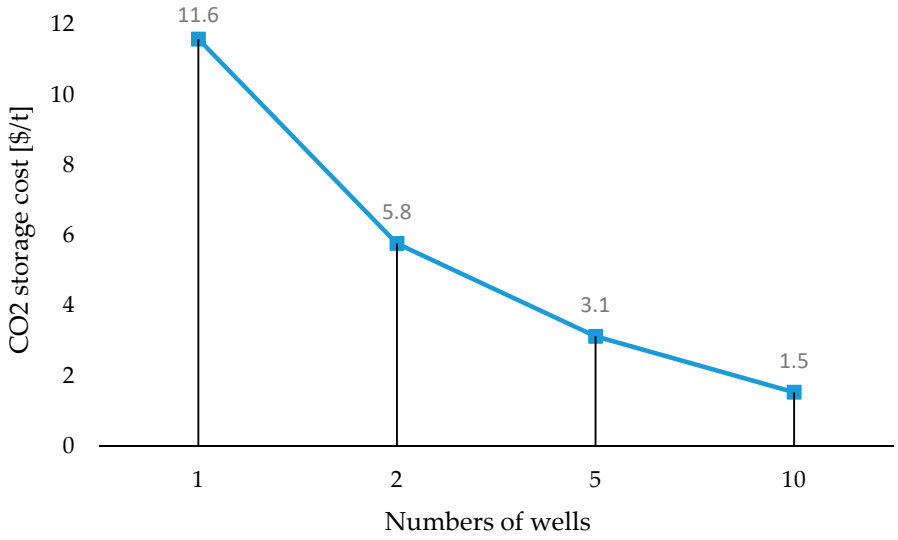

Figure 14. CO_2 storage cost at different numbers of wells when a combined method that includes CO_2 replacement and depressurisation of the NGH reservoir is applied to produce methane.

Increasing the number of wells, the revenue derived from methane's sale goes up because the methane production increases. Simultaneously, the amount of carbon dioxide that replaces the methane and is sequestrated as hydrate increases. As a result, the CO_2 storage cost drops from 11.6 $/t to 5.8 $/t when the wells' numbers pass from one to two, respectively. The minimum CO_2 storage cost was obtained with ten wells, but there are no manuscripts that report many such wells working simultaneously to produce methane in the NGH reservoir. Therefore, the CO_2 storage cost in NGH with two wells might be the representative value to compare this solution with the other possible storage sites.

Costs for geological storage are widely variable due to different reservoir types (e.g., onshore, offshore, depleted field, deep saline formation) and reservoir geology (e.g., depth, permeability). Therefore, storage cost is reported as a range, and the data are provided by different literature.

5.3. Methane Upgrade with Membrane-Based Separation Technology

Concerning the CO_2 separation process, membrane technology is used to upgrade biogas, increasing methane content on NG/SNG, reaching the purity fixed by a gas network.

Natural gas is considered a helpful bridge fuel to decrease greenhouse gas emissions. Purification and quality upgrade are necessary to use several natural gas reservoirs at low methane concentration as well as several processes are enough to carbon conversion and SNG production. For this purpose, membrane technology is applied to separate CH_4 from a mixture of gases composed by CO_2, CH_4, N_2, H_2O, and heavy hydrocarbons.

Commonly used glassy polymers for gas separation are polyimides (PI), polysulfone (PSF), polycarbonates (PC), while the mainly used rubber membranes are polyurethane (PU) and polydimethylsiloxane (PDMS). Among the PI polymers, Matrimid membranes are the most interesting; it is inflexible, strong and presents a CO_2 permeability of 12.7 barrer and CO_2/CH_4 ideal selectivity near to 40, at 20 bar [61].

PSF membranes are produced in three ways (asymmetric, dense, and composite), and they have CO_2 and CH_4 permeability of 12.33 and 4.69, respectively, while the CO_2/CH_4 selectivity is equal to 3.37 [62]. Carbon dioxide sequestration is relevant nowadays, and PDMS membranes possess excellent CO_2 permeability, high thermal stability, and a low rate of aging.

Also, the mixed matrix membrane is used to upgrade natural gas. Graphene oxide (GO) has been incorporated into the polyethylene oxide matrix (PEO) for sustainable CO_2 capture obtaining mechanical properties improvement. Permeability is enhanced by taking advantage of increased fractional free volume. As the GO contents increase from 0 to

1.0%wt, the H_2, N_2, and CO_2 (10 atm) permeabilities increase from 27.3, 5.84, and 280 barrer to 47.7, 8.5 and 474 barrer, respectively [63].

Simultaneous improvement in CO_2 permeability and CO_2/CH_4 selectivity can result in dispersing NOTT-300, a new MOF, in the Pebax1657 matrix. Increasing the content of BOF CO_2 permeability reached 395 barrer, while CO_2/N_2 and CO_2/CH_4 selectivity reached 61 and 36, respectively, at 10 bar [64].

Several authors have analysed the techno-economic feasibility of CO_2 removal from natural gas via membrane technology, more of them with a CO_2 content between 10% and 50% into the syngas. Yunhan Chu et al. have performed an HYSYS simulation and a cost evaluation. Assuming that 100 \$/m^2 is the carbon-based membrane cost, the use of two-stage with recycling and a feed syngas with 50% of CO_2, the natural gas processing cost results in 0.044 \$/Nm^3 of natural gas achieving 98% of CH_4 in the retentate and 2% of losses [65].

Gilassi et al. have performed a new optimization model to determine the optimum module number while minimizing the cost. The model has revealed that the use of two membrane units is enough to rich a pure output stream composed up to 98% of methane and reduce the methane losses above one percent. The biogas separation cost increases almost linearly with the content of CO_2 into the feed syngas. The biogas separation cost varies from 0.045 \$/Nm^3 to 0.09 \$/Nm^3 of CH_4 with 10% and 40% of CO_2 contents in the feed syngas, respectively [66].

The syngas produced during the methane extraction and simultaneous carbon dioxide sequestration from the NGH reservoir might contain 64% of CO_2. This value is higher than that estimated by the authors previously cited. Nevertheless, a two-stage membrane separation process to upgrade the methane content until 98% can also be used for this application, as shown in Figure 15. As a result, the separation cost can be equal to 0.126 \$/Nm^3 with 64% of CO_2 from its linearization. Therefore, the CO_2 separation cost is 0.036 \$/ton of CO_2 as evaluated in Equation (10).

$$C_{CO_2} = C_{syngas} \left[\frac{\$}{\mathrm{Nm}^3 CH_4}\right] * \frac{y_{CH_4}}{y_{CO_2} * \rho_{CO_2}} \left[\frac{\$}{t_{CO_2}}\right] \quad (10)$$

C_{CO_2} is the cost to separate the CO_2 in \$/ton of CO_2, C_{syngas} is the biogas separation cost, y_{CH_4} and y_{CO_2} are the mole fractions of methane and carbon dioxide in the syngas, respectively, and ρ_{CO_2} is the density of carbon dioxide equal to 1.976 ton/Nm^3 of CO_2.

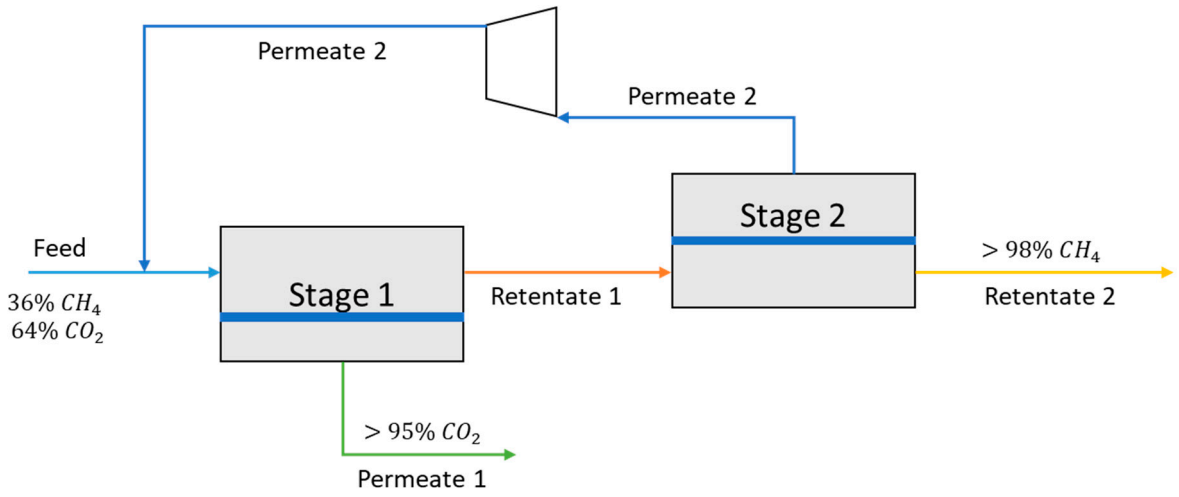

Figure 15. Membrane process for natural gas sweetening produced via depressurisation and CO_2 replacement.

6. Comparison between the Most Promising Technologies and CCS Cost Results

Previous sections present techno-economic analysis on the full pathway that, starting from captured CO_2 from power and process industries by several carbon capture technologies, will deliver it to geological sequestration by pipeline. The main carbon capture processes (oxyfuel-combustion, pre-combustion and post-combustion), the CO_2 transportation to onshore/offshore storage sites, the CO_2 deep marine injection into hydrates site are examined by techno-economic analysis. At the same time, several membranes with the best performance are reported for the purification of the CO_2/CH_4 effluent returning from the storage site in which injected CO_2 replaces CH_4.

The final CCS chain can be designed considering parameter specification of each component (capture, transport, and storage), incorporating relevant global parameters (e.g., electricity price, methane price) and evaluating economic outcomes of the chain, typically net present value and CO_2 cost. The potential of a commercial CCS project is affected by CCS technology maturity level, business economy factors, environmental impact risk associated with the full pathway of CCS, public acceptance, regulation, and market.

We have reported the efficiency penalty of the plant with CCS, the increasing levelized cost of electricity, and CO_2 capture cost. As key results, the cost of CO_2 captured for oxyfuel combustion (air separation unit), pre-combustion (PSA) and post-combustion (MEA) were 52 [$/t], 63 [$/t] and 46 [$/t], respectively, while the CO_2 capture cost resulted by membrane separation technology developed by MTR and NETL is 2 $/$t_{CO2}$ less than MEA. Therefore, the best performance is reached by applying the membrane separation process as post-combustion capture technology resulting in cheaper CO_2 capture cost. At the state of the art, MEA technology is the most used and less expansive at large scale, but the membrane capture system seems the most promising and interesting process to scale-up.

Concerning the transportation of CO_2, economic analysis shows different results when different methods are applied. Among them, we have illustrated the two, which lead to lower and higher values, to report the range of CO_2 cost transportation at different lengths of the pipeline. As result, for 100 [km], the range of CO_2 cost transportation is between 0.8 and 1.4 [$/t].

Finally, several geological storages were analyzed, and several values are reported in the literature. The biogas separation cost has to be added when methane is produced from a NGH reservoir.

Figure 16 points out the cost of the complete CCS chain, considering conventional storage sites and NGH reservoir. CCS cost low line is composed of the cost of CO_2 capture and the most economical cost of CO_2 transport (using Rui et al. method) and storage (1.5 $/t CO_2 see Table 8). On the contrary, the CCS cost high line takes into account the CO_2 capture cost, and the higher cost of CO_2 transport (using the Parker method) and storage (i.e., 30.6 $/t and 11.6 $/t for conventional site and NGH reservoir, respectively). The figure illustrates the trend of CCS cost at different distances between source and storage. As a result, the maximum price of CCS chains using membrane based-gas separation technology for CO_2 capture and for storing the carbon dioxide in the NGH reservoir is lower than the value of the CCS chain when the CO_2 is stored in a conventional site. The range of CCS cost at different pipeline length was evaluated, finding for CO_2 store in conventional reservoir and in NGH site [46.3;76] and [46.3;57] [$/t], respectively at 100 km.

The CO_2 capture is the most impacting cost item, as shown in Figure 17. This figure illustrates to what extent each step of the CCS chain affects the total cost at different pipeline length. It seems very clear that the CO_2 transportation is almost neglected for low distance, while capture and storage processes play a fundamental role in the CCS chain. As a result, for 100 km between source and NGH storage site, CO_2 capture with membrane technology, transport, and storage make up 86%, 2%, and 11%, respectively, of the total CCS cost.

Table 8. Range of storage cost for several reservoir types, either onshore or offshore. All prices are reported in US dollars in 2013.

Reference	Reservoir Type	On/Off-Shore	Low	High	Unit
[67]	Depleted O&G field—reusing wells	onshore	1.5	10.7	[$/t CO_2]
	Depleted O&G field—no reusing wells	onshore	1.5	15.3	[$/t CO_2]
	Saline formation	onshore	3.1	18.4	[$/t CO_2]
	Depleted O&G field—reusing wells	offshore	3.1	13.8	[$/t CO_2]
	Depleted O&G field—no reusing wells	offshore	4.6	21.4	[$/t CO_2]
	Saline formation	offshore	9.2	30.6	[$/t CO_2]
[68]	Saline formation	Onshore	6.8	12.6	[$/t CO_2]
[69]	Poor and good reservoir properties	Onshore	6.2	13.4	[$/t CO_2]
	CO_2 storage in NGH reservoir	Offshore	1.5	11.6	[$/t CO_2]

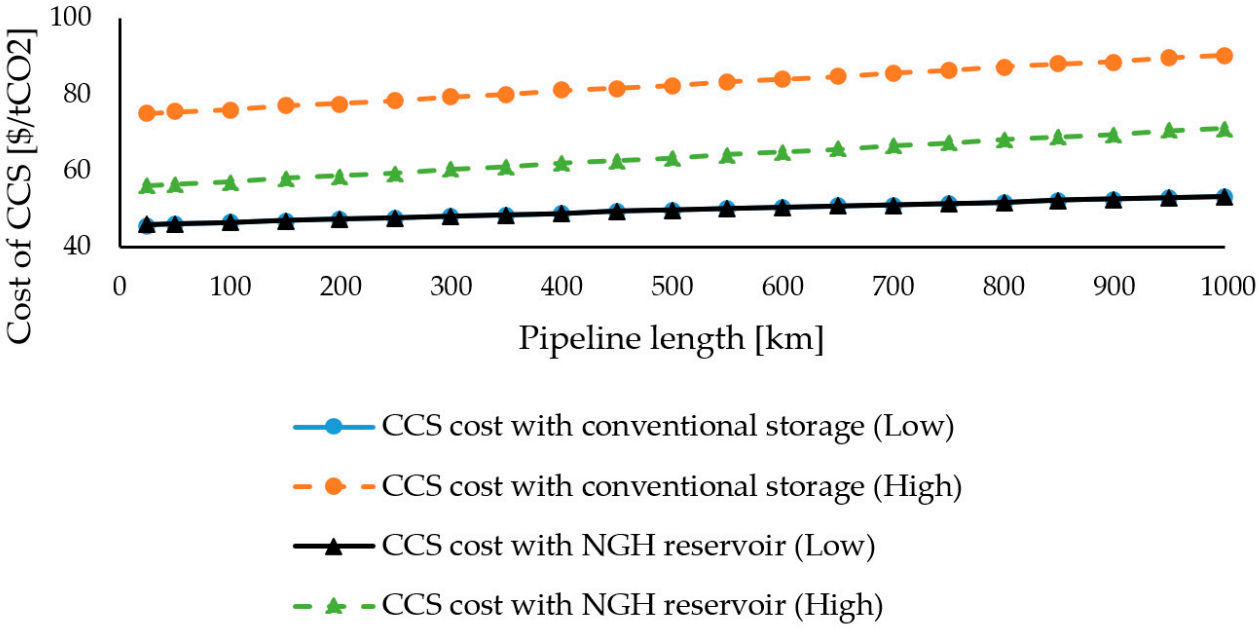

Figure 16. Cost of CCS at a different distance between source and storage. The continuous line represents the lower cost of CCS, while dashed lines are the higher value of CCS. The triangles indicate the CCS cost chain when methane is produced via depressurization and the CO_2 replacement, while the circles indicate the CCS cost chain with conventional storage sites described in Table 8.

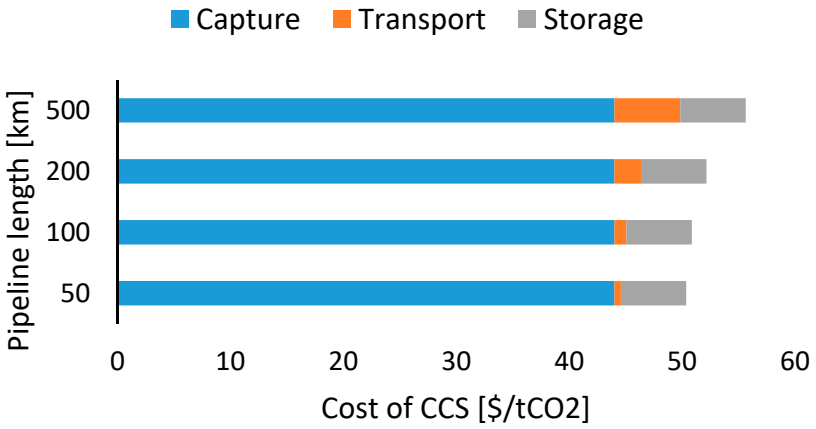

Figure 17. Total cost of CCS chain for several pipeline length, subdivided into the three components: capture, transportation, and storage in NGH. For the transportation cost was used a mean value while for the storage cost in NGH reservoir was assumed two wells.

The whole pathway of CO_2 is shown in Figure 18. The exhaust gas coming from a carbon-intensive plant is pre-treated into a CO_2 separation unit. The best performance technologies are the MEA process and the membrane capture process. The CO_2 captured is sent to the NGH reservoir through the pipeline transportation system, both onshore and offshore. The CO_2 transported before is injected into the NGH reservoir, thermodynamic condition changes, and syngas pass from hydrate to the gas phase. The produced syngas has to be treated in order to respect the regulations of the methane network. One of the best technologies to separate a gas mixture with CO_2/CH_4 is also the membrane separation technology.

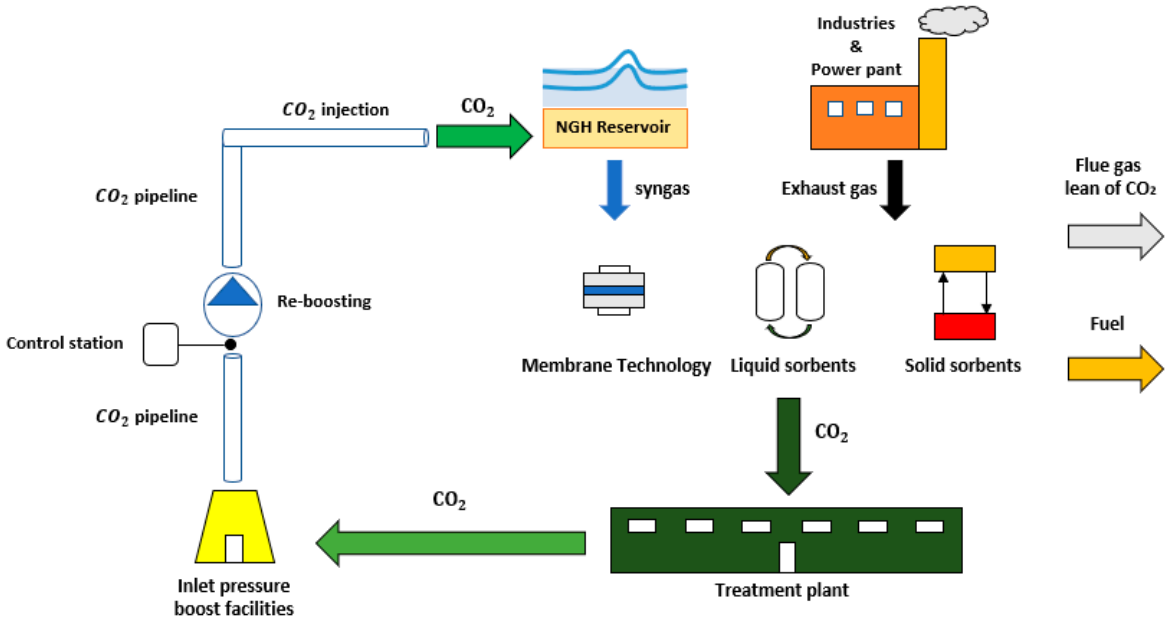

Figure 18. Final CCS chain. The flue gas from industries and power plants is treated into the separation unit. The CO_2 captured is transported via pipeline to the NGH reservoir. The injection of CO_2 causes a syngas production. The syngas was purified through membrane technology, and the permeant gas-rich of CO_2 will be injected another time in NGH reservoir. The fuel product rich of methane is in this way a neutral carbon fuel.

7. Conclusions

This paper explores options for CO_2-enhanced methane recovery from hydrates and clarifies the weight of each step on the overall CCS pathway. The main goal is to find the total cost of CCS to capture, transport, and store the CO_2 in the hydrate phase, replacing the natural gas produced from NGHs reservoir.

A wide range of CO_2 capture technologies are developed but there are only two large scale facility in operation configured to operate with MEA capture process. Several power plants equipped with different and promising carbon capture technologies have been built in order to reduce the CO_2 capture cost by learning from experience and meets a sufficient abatement of the CO_2 emission.

We have focused our study in one innovative capture technology, reporting membrane capture technology using the PoarisTM membrane developed by MTR. The cooperation between MTR and the Department of Energy (DOE)/NETL can help this technology became cheaper. The upgrade to plant scale is already programmed and could lead to reducing the CCS cost.

Successively, we have shifted the study on the CO_2 transportation from source to sink. To find the cost of CO_2 transportation, the NETL techno-economic model was used, resulting in optimal inner diameter and number of boost station. Pipeline transportation process is a mature technology but a new network that connect sources (i.e., power plants

and industries) with CO_2 consumers and storage sites should be implemented and financed by states.

The cost of CO_2 storage in the NGH reservoir was evaluated, but this process requires new experimental tests both at laboratory and in a real reservoir. Natural gas was produced through the injection of anthropogenic CO_2 in the NGH reservoir combined with a depressurization method. Future works will have the aim to find the CO_2 cost separation from syngas outgoing NGH. The membrane-based CO_2 separation process seems the best option to upgrade the methane stream, and new works are needed to develop membranes with higher permeability and selectivity useful for this process.

Funding: This research was funded by Ministry of Instruction, University and Research (MIUR), grant number 20173K5L3K, in the framework of the Research Project of Relevant National Interest (PRIN) called "Methane recovery and carbon dioxide disposal in natural gas hydrate reservoirs".

Institutional Review Board Statement: Not applicable.

Informed Consent Statement: Not applicable.

Data Availability Statement: Data available on request due to privacy restrictions. The data presented in this study are available on request from the corresponding author.

Acknowledgments: The authors gratefully acknowledge the supports of the Ministry of Instruction, University and Research (MIUR), grant number 20173K5L3K, in the framework of the Research Project of Relevant National Interest (PRIN) called "Methane recovery and carbon dioxide disposal in natural gas hydrate reservoirs".

Conflicts of Interest: The authors declare no conflict of interest.

Nomenclature

ASU	Air Separation Unit
BF	Blast Furnace
BOF	Basic Oxygen Furnace
CCS	Carbon capture and storage
CEPCI	Chemical Engineering Plant Cost Index
CPU	CO_2 Processing Unit
DOE	Department Of Energy
DRI	Direct Reduction Iron
EAF	Electric Arc Furnace
EOR	Enhanced Oil Recovery
ESP	Electro-Static Precipitator
FGD	Flue Gas Desulphurisation
FOAK	First-Of-A-Kind
FPU	Floating Production Unit
GDP	Gross Domestic Product
GO	Graphene oxide
GPU	Gas Permeation Unit
Gt	Giga tons
HHV	*Higher Heating Value*
HRSG	Heat Recovery Steam Generator
IGCC	Integrated Gasification Combined Cycle
IPCC	Intergovernmental Panel on Climate Change
LCOE	Levelized Cost Of Electricity
LEILAC	Low Emissions Intensity Lime and Cement
MAS ^{13}C NMR	Magic Angle Spinning Carbon-13 Nuclear Magnetic Resonance
MEA	Mono-ethanolamine
MIUR	Ministry of Education, University and Research
MMMs	Mixed Matrix Membranes
MOF	Metal-Organic Framework

MTR	Membrane and Technology Research
MW	Net Plant Capacity
NETL	National Energy Technology Laboratory
NG	Natural Gas
NGH	Natural gas hydrate
PC	polycarbonates
PCCI	Power Capital Cost Index
PDMS	polydimethylsiloxane
PEO	polyethylene oxide
PI	polyimides
PM	Particulate Matter
PRIN	Project of Relevant National Interest
PSA	Pressure Swing Absorption
PSF	Poly-sulfone
PU	polyurethane
ROW	Right-Of-Way
SCPC	Super-Critical Pulverised Coal
SNG	Synthetic Natural Gas
SOFC	Solid Oxide Fuel Cell
SR	Steam Reformer
TCC [$]	Total Capital Cost
tLS	ton of liquid steel
TRL	Technology Readiness Level
USC	Ultra-Super-Critical
VPSA	Vacuum Pressure Swing Absorption
WGS	Water Gas Shift
Parameters	
C	Capture fraction
C_{CO_2} [$/t]	CO_2 separation cost
C_{syngas} $[\frac{\$}{\mathrm{Nm}^3 CH_4}]$	Syngas separation cost
CF	capacity factor
f	CO_2 capture rate
FC [$/MJ]	Fuel Cost
FCF [fraction/year]	Fixed Charge Factor
FOM [$/y]	Fixed Operating and Maintenance cost
HR [MJ/MWh]	Heat Rate
$n_{CO_2\ injected}$	Mole of CO_2 injected
$n_{CO_2\ stored}$	Mole of CO_2 permanently stored
P_{eq} [MPa]	Equilibrium pressure
$Q_{e,b}$ [tCO_2/MWh]	Baseline emissions
R [J/(mol K]	specific gas constant
T [K]	Temperature
VOM [$/MWh]	Variable non-fuel Operating and Maintenance cost
W [J/mol]	Energy requirement
x	Molar Fraction on feed side
y	Molar Fraction on permeate side
α	Selectivity
η_b [%]	Baseline efficiency
η_{CC} [%]	Efficiency with carbon capture
η_{storage} [%]	Storage efficiency
ρ_{CO_2} $\left[\frac{\mathrm{t}}{\mathrm{Nm}^3}\right]$	CO_2 density

References

1. Masson-Delmotte, V.; Zhai, P.; Pörtner, H.O.; Roberts, D.; Skea, J.; Shukla, P.R.; Pirani, A.; Moufouma-Okia, W.; Péan, C.; Pidcock, R.; et al. Summary for Policymakers. *In Global Warming of 1.5 °C*. Available online: https://www.asme.org/about-asme/engineering-history/landmarks/228-philo-6-steam-electric-generating-unit (accessed on 11 January 2021).
2. IEA. *Global Energy & CO_2 Status Report 2019*; IEA: Paris, France, 2019.
3. Green, D.W.; Perry, R.H. *Perry's Chemical Engineers' Handbook*, 8th ed.; McGraw Hill Professional; McGraw-Hill Education: New York, NY, USA, 2007; ISBN 9780071593137.
4. IPCC Working Group III. *Climate Change 2014: Mitigation of Climate Change*; IPCC: Cambridge, UK, 2014.
5. MIT. *The Future of Natural Gas*; MIT: Cambridge, MA, USA, 2011.
6. Sloan, E.D. Fundamental principles and applications of natural gas hydrates. *Nature* **2003**, *426*, 353–359. [CrossRef] [PubMed]
7. Plecher, H. Share of Economic Sectors in the Global Gross Domestic Product (GDP) from 2007 to 2017. Available online: https://www.statista.com/statistics/256563/share-of-economic-sectors-in-the-global-gross-domestic-product/ (accessed on 11 January 2021).
8. IEA. *Global CO_2 Emissions by Sector, 2017*; IEA: Paris, France, 2017.
9. Lehne, J.; Preston, F. Making Concrete Change Innovation in Low-carbon Cement and Concrete. Available online: https://reader.chathamhouse.org/making-concrete-change-innovation-low-carbon-cement-and-concrete# (accessed on 11 January 2021).
10. Low Emission Intensity Lime and Cement (LEILAC). Public LEILAC Feed Summary Report. Available online: https://ec.europa.eu/research/participants/documents/downloadPublic?documentIds=080166e5b41458ac&appId=PPGMS (accessed on 11 January 2021).
11. World Steel Association Our Indicators. Available online: https://www.worldsteel.org/steel-by-topic/sustainability/sustainability-indicators.html (accessed on 11 January 2021).
12. The World Steel Association. World Steel in Figures 2019. 2019. Available online: https://www.worldsteel.org/en/dam/jcr:96d7a585-e6b2-4d63-b943-4cd9ab621a91/World%2520Steel%2520in%2520Figures%25202019.pdf (accessed on 11 January 2021).
13. Paoluzzi, D.; Martinis, A.; Danieli & Office Meccaniche. Sustainable Decrease of CO_2 Emissions in the Steelmaking Industry by Means of the Energiron Direct Reduction Technology. Available online: http://keepmoving.com.mx/kmt-test/energirondemouno/wp-content/uploads/2019/07/Environmental-sustainability-80-CO2-emissions-achievable.pdf (accessed on 11 January 2021).
14. ASME. 228 Philo 6 Steam-Electric Generating Unit. Available online: https://www.asme.org/about-asme/engineering-history/landmarks/228-philo-6-steam-electric-generating-unit (accessed on 11 January 2021).
15. IEA. *Technology Roadmap—High-Efficiency, Low-Emissions Coal-Fired Power Generation*; IEA: Paris, France, 2012.
16. Tan, X. Supercritical and ultrasupercritical coal-fired power generation. *Bus. Public Adm. Stud.* **2012**, *7*, 53.
17. Stéphenne, K. Start-up of World's First Commercial Post-combustion Coal Fired CCS Project: Contribution of Shell Cansolv to SaskPower Boundary Dam ICCS Project. *Energy Procedia* **2014**, *63*, 6106–6110. [CrossRef]
18. Vega, F.; Baena-Moreno, F.M.; Gallego Fernández, L.M.; Portillo, E.; Navarrete, B.; Zhang, Z. Current status of CO_2 chemical absorption research applied to CCS: Towards full deployment at industrial scale. *Appl. Energy* **2020**, *260*, 114313. [CrossRef]
19. Amel'kin, S.A.; Burtzler, J.M.; Hoffmann, K.H.; Tsirlin, A.M. Evaluating the Efficiency Frontier of Separation Processes. *Theor. Found. Chem. Eng.* **2001**, *35*, 217–223. [CrossRef]
20. Budinis, S.; Krevor, S.; Mac Dowell, N.; Brandon, N.; Hawkes, A. An assessment of CCS costs, barriers and potential. *Energy Strateg. Rev.* **2018**, *22*, 61–81. [CrossRef]
21. Rubin, E.S.; Davison, J.E.; Herzog, H.J. The cost of CO_2 capture and storage. *Int. J. Greenh. Gas Control* **2015**, *40*, 378–400. [CrossRef]
22. Merkel, T.; Kniep, J.; Wei, X.; Carlisle, T.; White, S.; Pande, S.; Fulton, D.; Watson, R.; Hoffman, T.; Freeman, B.; et al. *Pilot Testing of a Membrane System for Postcombustion CO_2 Capture*; Membrane Technology and Research, Incorporated: Newark, CA, USA, 2015.
23. Stanger, R.; Wall, T.; Spörl, R.; Paneru, M.; Grathwohl, S.; Weidmann, M.; Scheffknecht, G.; McDonald, D.; Myöhänen, K.; Ritvanen, J.; et al. Oxyfuel combustion for CO_2 capture in power plants. *Int. J. Greenh. Gas Control* **2015**, *40*, 55–125. [CrossRef]
24. Mathieu, P. Oxyfuel combustion systems and technology for carbon dioxide (CO_2) capture in power plants. In *Developments and Innovation in Carbon Dioxide (CO_2) Capture and Storage Technology*; Woodhead Publishing: Cambridge, UK, 2010; pp. 283–319. [CrossRef]
25. Wang, G.; Ma, Z.; Deng, J.; Li, Z.; Duan, L.; Zhang, Q.; Hao, J.; Jiang, J. Characteristics of particulate matter from four coal–fired power plants with low–low temperature electrostatic precipitator in China. *Sci. Total Environ.* **2019**, *662*, 455–461. [CrossRef]
26. Córdoba, P. Status of Flue Gas Desulphurisation (FGD) systems from coal-fired power plants: Overview of the physic-chemical control processes of wet limestone FGDs. *Fuel* **2015**, *144*, 274–286. [CrossRef]
27. IEAGHG. Towards Zero Emissions CCS in Power Plants Using Higher Capture Rates or Biomass. Available online: https://climit.no/wp-content/uploads/sites/4/2019/09/IEAGHG-Report-2019-02-Towards-zero-emissions.pdf (accessed on 11 January 2021).
28. Schiebahn, S.; Grube, T.; Robinius, M.; Zhao, L.; Otto, A.; Kumar, B.; Weber, M.; Stolten, D. Power to Gas. In *Transition to Renewable Energy Systems*; John Wiley & Sons, Ltd.: Hoboken, NJ, USA, 2013; pp. 813–848. ISBN 9783527673872.

29. Desideri, U. Advanced absorption processes and technology for carbon dioxide (CO_2) capture in power plants. In *Developments and Innovation in Carbon Dioxide (CO_2) Capture and Storage Technology*; Woodhead Publishing: Cambridge, UK, 2010; pp. 155–182. [CrossRef]
30. Shimizu, T.; Hirama, T.; Hosoda, H.; Kitano, K.; Inagaki, M.; Tejima, K. A Twin Fluid-Bed Reactor for Removal of CO_2 from Combustion Processes. *Chem. Eng. Res. Des.* **1999**, *77*, 62–68. [CrossRef]
31. Cannone, S.F.; Stendardo, S.; Lanzini, A. Solar-powered Rankine cycle assisted by an innovative calcium looping process as energy storage system. *Ind. Eng. Chem. Res.* **2020**, *59*, 6977–6993. [CrossRef]
32. Bui, M.; Adjiman, C.S.; Bardow, A.; Anthony, E.J.; Boston, A.; Brown, S.; Fennell, P.S.; Fuss, S.; Galindo, A.; Hackett, L.A.; et al. Carbon capture and storage (CCS): The way forward. *Energy Environ. Sci.* **2018**, *11*, 1062–1176. [CrossRef]
33. Calabrò, V.; Iulianelli, A.; Liguori, S.; Basile, A.; Gugliuzza, A.; Saraceno, A. State of the Art on CO_2 Separation Processes with Membrane Technology (In Italian). Available online: https://www.enea.it/it/Ricerca_sviluppo/documenti/ricerca-di-sistema-elettrico/celle-a-combustibile-biomasse/rds-139-2.1.2-stato-dell2019arte-sui-processi-di-rimozione.pdf (accessed on 11 January 2021).
34. Credence Research Gas Separation Membranes market, by Type, Application and Region—Growth, Future Prospects and Competitive Analysis. Available online: https://www.credenceresearch.com/report/gas-separation-membranes-market (accessed on 11 January 2021).
35. Aroon, M.A.; Ismail, A.F.; Matsuura, T.; Montazer-Rahmati, M.M. Performance studies of mixed matrix membranes for gas separation: A review. *Sep. Purif. Technol.* **2010**, *75*, 229–242. [CrossRef]
36. IEA. *Energy Technology Perspectives 2012*; IEA: Paris, France, 2012.
37. Luo, X.; Wang, M.; Oko, E.; Okezue, C. Simulation-based techno-economic evaluation for optimal design of CO_2 transport pipeline network. *Appl. Energy* **2014**, *132*, 610–620. [CrossRef]
38. Intergovernmental Panel on Climate Change (IPCC). Carbon Dioxide Capture and Storage. Available online: https://www.ipcc.ch/site/assets/uploads/2018/03/srccs_wholereport.pdf (accessed on 11 January 2021).
39. Woodhill Engineering Consultants. Pipeline Transmission of CO_2 and Energy. Transmission Study Report. Prepared by Woodhill Engineering Consultants; IEA GHG. Report No.: PH4/6. 2002. Available online: https://ieaghg.org/docs/General_Docs/Reports/PH4_6%20TRANSMISSION%20REPORT.pdf (accessed on 11 January 2021).
40. Onyebuchi, V.E.; Kolios, A.; Hanak, D.P.; Biliyok, C.; Manovic, V. A systematic review of key challenges of CO_2 transport via pipelines. *Renew. Sustain. Energy Rev.* **2018**, *81*, 2563–2583. [CrossRef]
41. Knoope, M.M.J.; Ramírez, A.; Faaij, A.P.C. A state-of-the-art review of techno-economic models predicting the costs of CO_2 pipeline transport. *Int. J. Greenh. Gas Control* **2013**, *16*, 241–270. [CrossRef]
42. National Energy Technology Laboratory (NETL). *FE/NETL CO_2 Transport Cost Model: Description and User's Manual*; NETL: Pittsburgh, PA, USA, 2018.
43. Parker, N. *Using Natural Gas Transmission Pipeline Costs to Estimate Hydrogen Pipeline Costs*; Institute of Transportation Studies: UC Davis, CA, USA, 2004.
44. McCoy, S.T.; Rubin, E.S. An engineering-economic model of pipeline transport of CO_2 with application to carbon capture and storage. *Int. J. Greenh. Gas Control* **2008**, *2*, 219–229. [CrossRef]
45. Rui, Z.; Metz, P.; Reynolds, D.; Chen, G.; Zhou, X. Regression models estimate pipeline construction costs. *Oil Gas J.* **2011**, *109*, 120–127.
46. Thomas, S. Enhanced Oil Recovery—An Overview. *Oil Gas Sci. Technol. Rev. IFP* **2008**, *63*, 9–19. [CrossRef]
47. White, M.; McGrail, P. Designing a pilot-scale experiment for the production of natural gas hydrates and sequestration of CO_2 in class 1 hydrate accumulations. *Energy Procedia* **2009**, *1*, 3099–3106. [CrossRef]
48. Kondori, J.; Zendehboudi, S.; Hossain, M.E. A review on simulation of methane production from gas hydrate reservoirs: Molecular dynamics prospective. *J. Pet. Sci. Eng.* **2017**, *159*, 754–772. [CrossRef]
49. Uchida, T.; Ikeda, I.Y.; Takeya, S.; Kamata, Y.; Ohmura, R.; Nagao, J.; Zatsepina, O.Y.; Buffett, B.A. Kinetics and stability of CH_4-CO_2 mixed gas hydrates during formation and long-term storage. *Chemphyschem* **2005**, *6*, 646–654. [CrossRef] [PubMed]
50. Le, Q.-D.; Rodriguez, C.T.; Legoix, L.N.; Pirim, C.; Chazallon, B. Influence of the initial CH4-hydrate system properties on CO_2 capture kinetics. *Appl. Energy* **2020**, *280*, 115843. [CrossRef]
51. McGrail, B.P.; Schaef, H.T.; White, M.D.; Zhu, T.; Kulkarni, A.S.; Hunter, R.B.; Patil, S.L.; Owen, A.T.; Martin, P.F. *Using Carbon Dioxide to Enhance Recovery of Methane from Gas Hydrate Reservoirs: Final Summary Report*; Pacific Northwest National Lab. (PNNL): Richland, WA, USA, 2007.
52. Lee, H.; Seo, Y.; Seo, Y.-T.; Moudrakovski, I.L.; Ripmeester, J.A. Recovering Methane from Solid Methane Hydrate with Carbon Dioxide. *Angew. Chem. Int. Ed.* **2003**, *42*, 5048–5051. [CrossRef] [PubMed]
53. Adisasmito, S.; Frank, R.J.; Sloan, E.D. Hydrates of carbon dioxide and methane mixtures. *J. Chem. Eng. Data* **1991**, *36*, 68–71. [CrossRef]
54. Goel, N. In situ methane hydrate dissociation with carbon dioxide sequestration: Current knowledge and issues. *J. Pet. Sci. Eng.* **2006**, *51*, 169–184. [CrossRef]
55. Clennell, M.B.; Hovland, M.; Booth, J.S.; Henry, P.; Winters, W.J. Formation of natural gas hydrates in marine sediments 1. Conceptual model of gas hydrate growth conditioned by host sediment properties. *J. Geophys. Res. B Solid Earth* **1999**, *104*, 22985–23003. [CrossRef]

56. Gambelli, A.M.; Castellani, B.; Nicolini, A.; Rossi, F. Experimental study on natural gas hydrate exploitation: Optimization of methane recovery, carbon dioxide storage and deposit structure preservation. *J. Pet. Sci. Eng.* **2019**, *177*, 594–601. [CrossRef]
57. Zhao, J.; Zhang, L.; Chen, X.; Zhang, Y.; Liu, Y.; Song, Y. Combined replacement and depressurization methane hydrate recovery method. *Energy Explor. Exploit.* **2016**, *34*, 129–139. [CrossRef]
58. Yu, T.; Guan, G.; Abudula, A.; Yoshida, A.; Wang, D.; Song, Y. Gas recovery enhancement from methane hydrate reservoir in the Nankai Trough using vertical wells. *Energy* **2019**, *166*, 834–844. [CrossRef]
59. Vedachalam, N.; Ramesh, S.; Jyothi, V.B.N.; Ramadass, G.A.; Atmanand, M.A.; Manivannan, P. Techno-economic viability studies on methane gas production from gas hydrates reservoir in the Krishna-Godavari basin, east coast of India. *J. Nat. Gas Sci. Eng.* **2020**, *77*, 103253. [CrossRef]
60. Natural Gas Prices in Selected Markets from 2017 to 2030 (in Nominal U.S. Dollars per Million British Thermal Units). Available online: https://www.statista.com/statistics/444286/natural-gas-price-forecast-by-region/ (accessed on 11 January 2021).
61. De Angelis, M.G.; Giacinti Baschetti, M.; Minelli, M.; Olivieri, L.; Deiana, P.; Bassano, C. Synthesis, Characterization and Testing of CO_2 Separation Membranes and Purification of Synthetic Natural Gas (SNG) (In Italian). Available online: https://www.enea.it/it/Ricerca_sviluppo/documenti/ricerca-di-sistema-elettrico/combustibili-fossili-ccs/2014/rds-par2014-269.pdf (accessed on 11 January 2021).
62. Mohamad, M.B.; Shariff, A. Gas Separation of Carbon Dioxide from Methane Using Polysulfone Membrane Incorporated with Zeolite-T. *Procedia Eng.* **2016**, *148*, 621–629. [CrossRef]
63. Quan, S.; Li, S.W.; Xiao, Y.C.; Shao, L. CO_2-selective mixed matrix membranes (MMMs) containing graphene oxide (GO) for enhancing sustainable CO_2 capture. *Int. J. Greenh. Gas Control* **2017**, *56*, 22–29. [CrossRef]
64. Habib, N.; Shamair, Z.; Tara, N.; Nizami, A.-S.; Akhtar, F.H.; Ahmad, N.M.; Gilani, M.A.; Bilad, M.R.; Khan, A.L. Development of highly permeable and selective mixed matrix membranes based on Pebax®1657 and NOTT-300 for CO_2 capture. *Sep. Purif. Technol.* **2020**, *234*, 116101. [CrossRef]
65. Gilassi, S.; Taghavi, S.M.; Rodrigue, D.; Kaliaguine, S. Optimizing membrane module for biogas separation. *Int. J. Greenh. Gas Control* **2019**, *83*, 195–207. [CrossRef]
66. Chu, Y.; He, X. Process Simulation and Cost Evaluation of Carbon Membranes for CO_2 Removal from High-Pressure Natural Gas. *Membranes* **2018**, *8*, 118. [CrossRef]
67. ZEP. The Costs of CO_2 Storage: Post-Demonstration CCS in the EU. Available online: https://www.globalccsinstitute.com/archive/hub/publications/119816/costs-co2-storage-post-demonstration-ccs-eu.pdf (accessed on 11 January 2021).
68. USDOE. *CO_2 Saline Storage Cost Model: Model Description and Baseline Results*; USDOE: Pittsburgh, PA, USA, 2014.
69. GCCSI. *Economic Assessment of Carbon Capture and Storage Technologies*; GCCSI: Canberra, Australia, 2011.